



McGill

Faculty of
Medicine and
Health Sciences

Photobiomodulation in the near infrared and red spectra induces
nitric oxide release in ex-vivo human skin homogenate via
enzymatic pathways

by

Augustin C. Barolet

Experimental Surgery
McGill University, Montreal
April 2021

A thesis submitted to McGill University in partial fulfillment of the requirements of the degree of
Master of Science (M. Sc.)

© Augustin C. Barolet, 2021

Table of Content

Abstract	1
English Abstract	1
French Abstract	2
Acknowledgements	4
Contribution	4
Introduction	5
UVA-induced NO release	8
Key Absorption Spectra	9
Blue light induced NO release	13
Red/NIR light therapy: New contenders	15
NO Detection Methods in Tissues	20
Fluorophores.....	20
Confocal Microscopy	21
Chemiluminescence	22
Griess Assay	24
The Relevance of Light-induced NO Release in Human Skin.....	24
NO mobilization leads to Local & Systemic effects	24
NO Local Effects.....	25
NO Systemic Effects	26

Hypothesis and Aims	29
Methods.....	30
Table of Materials	30
Experimental design.....	32
Skin homogenate preparation.....	33
Skin homogenate incubation	33
Skin homogenate treatment.....	34
Griess reaction assay	37
Data analysis	38
Results	39
Results 1 – Light treatment vs. Sham experiment.....	39
Results 2 – L-NMMA control experiment	41
Results 3 – C-PTIO control experiment.....	42
Combined comparisons	43
Experiment 1 (only light treatment) vs. Experiment 2 (L-NMMA)	43
Experiment 1 (only light treatment) vs. Experiment 3 (C-PTIO)	44
Discussion	46
UVA exposure.....	47
Red and NIR exposure	48
Combined comparison.....	49

Clinical Aspects.....49

Next steps50

Conclusion.....50

Referencesi

Abstract

English Abstract

Background and Significance: Human skin can absorb light just like plants, and this absorption is far beyond ultraviolet (UV) radiation. Visible (400 – 700 nm) and near-infrared (IR-A: 700-1200 nm) spectra are also absorbed and may modulate cell signalling pathways beneficial to human skin. Nowadays, these spectra can be artificially reproduced using non-ionizing low-intensity light. This science, named Photobiomodulation (PBM), uses visible and IR-A light to modulate the cell's metabolism to self-correct, if necessary. At the cellular level, visible and IR-A absorption may also modulate the cell's nitric oxide (NO) metabolism. NO is a biomolecule omnipresent in the body that can be released enzymatically or photolytically in the skin. Localized NO content protects cells from oxidative stress and notably promotes wound healing. Circulating NO reduces blood pressure and can engender beneficial effects on distant organs. The use of red and IR-A to mobilize NO stores from the skin is auspicious.

Hypothesis and Objective: We hypothesized that the red and IR-A spectra have the potential to release cutaneous NO. We measured their effect using *ex vivo* human skin and compared them to positive control UVA. Finally, we evaluated the impact of NO synthases (NOSs) on cutaneous NO metabolism following light exposure to IR-A and red wavelengths.

Methods: The Griess colorimetric nitrite assay was used for the indirect quantitative determination of NO to assess our hypothesis. IR-A (850 nm) and red (660 nm) were compared to narrow band UVA (365 nm). Paired and unpaired t-test approaches were chosen as statistical tests to compare each group, and a 95% confidence interval was calculated for each condition's mean concentration in all experiments.

Result and Discussion: IR-A and red can release a significant amount of NO from our ex vivo human skin model when compared to sham group. As expected, our benchmark UVA released the highest amount of NO. NIR and red cellular impacts on NO metabolism seem to be related to enzymatic NOS modulation compared to UVA photolytic effects. The non-selective NOS inhibitor NG-monomethyl L-arginine (L-NMMA) abrogated most of the NIR-related NO release in our ex-vivo human skin model. The selective NO scavenger carboxyl-PTIO decreased the amount of NO release by all the wavelengths. Further studies are needed to elucidate the molecular pathways underlying light-based NO modulation in the skin.

French Abstract

Contexte et importance: La peau humaine peut absorber la lumière comme les plantes, et cette absorption va bien au-delà des rayons ultraviolets (UV). La lumière visible (400 – 700 nm) et l'infrarouge proche (IRP: 700-1200 nm) sont également absorbés et peuvent moduler les voies de signalisations cellulaires bénéfiques pour la peau humaine. De nos jours, ces spectres peuvent être reproduits artificiellement en utilisant des lumières non-ionisantes de faible intensité. Cette science, nommée Photobiomodulation (PBM), utilise la lumière visible et IRP pour moduler le métabolisme de la cellule afin qu'elle s'auto-corrige, si nécessaire. Au niveau cellulaire, l'absorption du rouge et d'IRP peuvent également moduler le métabolisme de l'oxyde nitrique (NO) dans la cellule. Le NO est une biomolécule omniprésente dans l'organisme qui peut être libérée par voie enzymatique ou photolytique. La haute teneur localisée en NO protège les cellules du stress oxydatif et favorise notamment la cicatrisation des plaies. Le NO circulant dans le corps peut aussi réduire la pression artérielle et engendre également des effets bénéfiques à distance dans certains organes éloignés de la source de libération. L'utilisation du rouge et de l'IRP pour mobiliser le vaste bassin d'NO dans la peau est très prometteur.

Hypothèse et objectif: Nous avons hypothétisé que le spectre du rouge et de l'IRP sont des excellents candidats pour libérer du NO dans la peau humaine. Nous avons mesuré leur effet sur un modèle de peau humaine ex vivo et les avons comparé au standard utilisant l'effet photolytique de l'UVA. Enfin, nous avons évalué l'impact des NO synthases (NOSs) sur le métabolisme cutané du NO suivant des traitements de rouge et d'IRP.

Méthodes: L'analyse de Griess Assay a été utilisée pour évaluer notre hypothèse sur un modèle de peau humaine ex vivo. Le rouge (660 nm) et l'IRP (850 nm) ont été comparés à l'UVA (365 nm). Pour comparer nos groupes, les approches de t-test apparié et non-apparié ont été utilisés comme tests statistiques. Aussi, un intervalle de confiance à 95% a été calculé pour la concentration moyenne de chaque condition.

Résultat et discussion: Le rouge et l'IRP peuvent libérer une quantité significative de NO à partir de notre modèle de peau humaine ex vivo. Comme prévu, l'UVA, notre contrôle positif, a émis la plus grande concentration de NO. La libération de NO découlant du rouge et de l'IRP semble être reliée aux effets enzymatiques des NOSs, spécialement pour l'IRP. L'inhibiteur non-sélectif des NOSs NG-monométhyl L-arginine (L-NMMA) a neutralisé la libération d'NO par le rouge et l'IRP contrairement aux contrôles. Le capteur moléculaire sélectif de NO carboxyl-PTIO a aboli la libération de NO pour toutes les longueurs d'onde utilisées dans cette expérimentation. D'autres études sont nécessaires pour élucider les voies moléculaires sous-jacentes à la libération et modulation du NO cutané par la lumière visible et IRP.

Acknowledgements

First and foremost, I would like to thank my thesis supervisor, Dr. Ivan V. Litvinov, for his wonderful guidance, help and enthusiasm throughout this project. Also, I would like to express my most sincere gratitude to my tutor Dr. Daniel Barolet. He has sacrificed much of his precious time in guiding and supporting me throughout my master's.

Moreover, many thanks to my fellow students of Litvinov lab at McGill University Health Centre for their support during these two years. Particularly, I would like to thank Jennifer Gantchev, Amelia Villareal Martinez, Brandon Ramchatesingh, and Scott Gun. Finally, I would like to thank Mathieu Auclair, of RoseLab Skin Optics Research Lab, for his constant assistance throughout my research projects.

Contribution

The work presented in this thesis is my own. I performed all the literature review, conception of custom reaction chamber, conception of lab module, lab procedures, data collection, and data analysis. All this work was done under Dr. Ivan V. Litvinov and Dr. Daniel Barolet's supervision.

Introduction

Nitric oxide (NO) is synthesized endogenously by Nitric Oxide Synthase (NOS), including three different types; two are expressed constitutively, and one is an inducible isozyme [1]. There are neuronal NOS (nNOS) along with endothelial (eNOS) and inducible NOS (iNOS). nNOS and eNOS have been discovered in their respective cell types and are constitutively expressed, as opposed to iNOS, which is inducibly expressed in a variety of human cells. The three NOSs have been detected in human skin [2], where NOS-dependent production of NO potentially occurring in all cell types driven by one or more of the three NOSs [3]. NOS isoenzymes are homodimeric proteins needing many cofactors to perform their catalytic activity, such as incorporating molecular oxygen to L-arginine to release NO and the formation of L-citrulline as an end-product. Those cofactors are nicotinamide adenine dinucleotide phosphate (NADPH), reduced flavins, heme-bound iron, and 6 (R) 5,6,7,8-tetrahydrobiopterin. Expression of nNOS has been identified in keratinocytes and melanocytes [4]. Mast cells located in the dermis also express nNOS [5]. Whereas eNOS can be observed in keratinocytes of the basal epidermal layer, dermal fibroblasts, endothelial cells, and eccrine glands. Generally, iNOS is not expressed in resting skin cells but maybe induced following immune / inflammatory activation. In pro-inflammatory skin environments, keratinocytes, fibroblasts, Langerhans cells, endothelial cells, and mast cells may express iNOS [6]. The constitutively expressed NOS isoforms, like nNOS and eNOS, are activated by increasing calcium influx levels leading to the activation of the NOS-upstream activator, calmodulin [4]. iNOS is unique among the NOS family in that it is not regulated by calcium signals; instead, it is continuously active once expressed [7]. Also, iNOS generates the highest concentrations of NO, which is in nanomolar rather than picomolar, and this level of synthesis is sustained for hours or longer until the enzyme is cleared from the cells or tissues [7].

NO is a free radical with an unpaired electron in his highest orbital state. It behaves as a potential antioxidant agent by reducing other molecules and therefore inhibits lipid peroxidation [8]. However, NO is quickly inactivated by the superoxide anion (O_2^-) to form peroxynitrite ($ONOO^-$), known as a potent oxidant [9]. As NO and O_2^- are simultaneously released by cells, the balance between these two radicals is decisive in the faith of NO towards lipid peroxidation. Hence, a higher NO/ O_2^- ratio will favor lipid peroxidation inhibition, while ratios equal or lower to 1 will induce lipid peroxidation [8].

The short half-life of NO (gaseous state) could explain the sphere of influence of this biomolecule and its limited diffusion in the immediate microenvironment. It is currently understood that NO can be stored in an accessible pool of compounds easily converted to NO [10]. Some proteins and biomolecules react quickly with NO, resulting in S-, N-, O-, and C- nitroso compounds, such as S-nitroso-glutathione (GS-NO) or S-nitroso-albumin [11]. In addition, oxygen reacts quickly with NO, forming nitrite (NO_2^-) and nitrate (NO_3^-). These NO derivatives can be found in relatively high skin concentrations, and some are easily converted to NO (Figure 1) [10, 12]. In fact, S- and N- nitroso compounds (RS-NO and RN-NO) along with other NO derivatives, like nitrite and nitrate, are found in high concentrations in the skin [13]. Concentrations of nitrite and RS-NO reach up to 15 μ M and 7 μ M in healthy subjects' skin, respectively. This represents 25- and 360- times the concentration of these respective compounds found in the plasma [13].

Following skin irradiation by Ultraviolet A (UVA) light, some studies showed that cutaneous stores of NO derivatives can be mobilized to the bloodstream [14]. They showed that UVA increased circulating nitrite and reduced circulating nitrate [14]. NO was therefore made more available, with nitrite easily converted to NO by UV irradiation, a reaction called UV photolysis [15-17]. So, UVA irradiation of the skin freed up some of its large stores of NO derivatives, making NO available to promote vasodilation and other biological processes. In other words, human skin contains NO

derivatives photodecomposed to NO following UVA irradiation and presumably independent of NOS involvement.

More recently, blue light has been shown to release NO [18, 19] into blood circulation coming from photolabile intracutaneous NO metabolites with corresponding cardiovascular benefits [20]. Longer wavelengths in the red and NIR spectra may also be used to release NO locally and systemically. Our group recently showed that by using red and NIR wavelengths, one could release NO non-enzymatically from ex-vivo skin [21, 22].

Low-intensity visible and NIR light is part of photobiomodulation (PBM). NO is one of the three PBM primary cellular effectors, namely ATP, ROS and NO. They can all be released by the mitochondria following photons' absorption by the main chromophore cytochrome c oxidase. NOSs have also been linked to red/NIR light-induced NO release [23]. Despite established ultraviolet radiation (UVR) and blue light photolytic release of NO in the skin [15, 24], light exposure in the red/NIR spectrum is a promising alternative using safer non-ionizing photons [21, 25]. NO stores are prominent and mostly located in the epidermis, modulating local and remote systemic effects [20]. Finding new methods to mobilize such a substantial NO reservoir in the skin have broad implications in photomedicine.

Herein, we will describe the current knowledge on light-induced NO release in the skin using UVR and blue light. We will also introduce new modalities capable of releasing NO in the red and near-infrared spectra, elaborate on commonly used NO detection methods and discuss relevant NO-related skin applications. Next, my masters' thesis research project measuring nitric oxide release (Griess assay) in *ex-vivo* human skin homogenate following UVA/red/near-infrared light exposure will be presented.

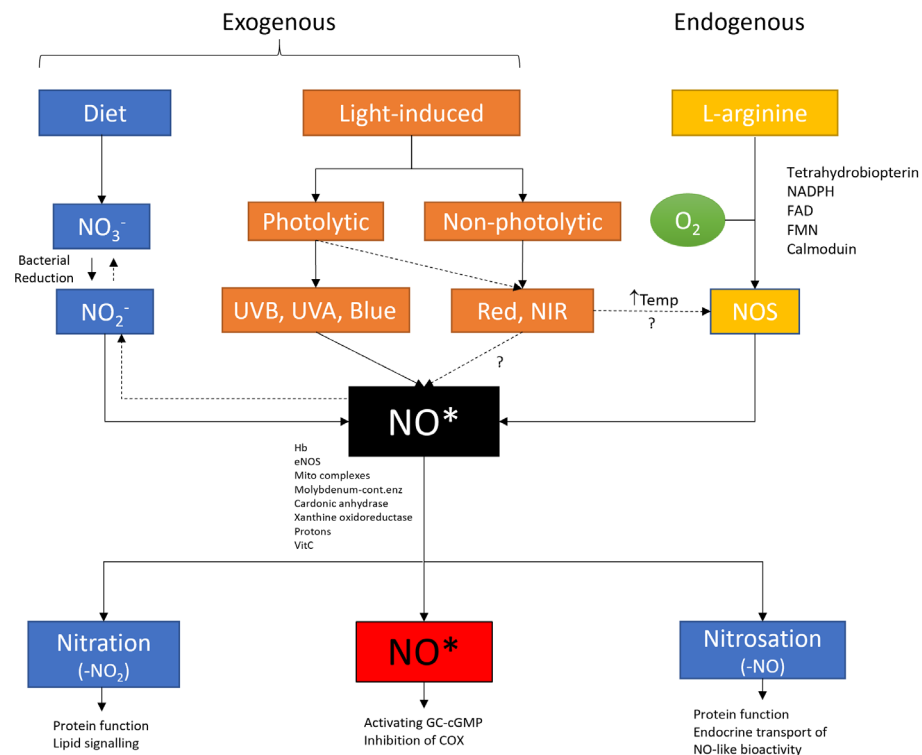


Figure 1. Major pathways lead to NO formation in the skin primarily originating from exogenous and endogenous sources and subsequent nitration/nitrosation metabolic end-reactions. Apart from dietary intake and endogenous stores of L-arginine, light-induced mobilization of NO is conceivable. Despite established NO release benefits via UVR and blue light, the use of longer wavelengths in the red/NIR spectrum remains to be determined. (O₂; oxygen, NO₃; nitrate, NO₂; nitrite, NOS; nitric oxide synthase, UVB; ultraviolet B, UVA; ultraviolet A, NIR; near-infrared, NO; nitric oxide)

UVA-induced NO release

Among several UVA-induced NO release studies [10, 26-32], Liu *et al.* demonstrated that there is a photolytic process occurring following human skin irradiation. [14]. This report showed that most of the light-sensitive NO pool (fluorescence) was located in the upper epidermis and stratum

corneum. Moreover, the reaction was unaffected by the NOS antagonist NG-monomethyl L-arginine (L-NMMA), but entirely abrogated by the NO scavenger cPTIO, suggesting that UVA photolytic effect can significantly release NO non-enzymatically. Another study showed the implication of UVA radiation in upregulating iNOS expression [33]. The results showed a peak in iNOS expression 24-hour post-UVA irradiation, and a return to normal levels after 72 hours. Furthermore, through epidermal growth factor (EGF) receptors, UVA induces a calcium influx in keratinocytes, which activates NOSs and the formation of ROS [11, 34]. Similarly, UVA is also known to modulate a calcium influx in melanocytes via the retinal-dependent pathway [35]. Additionally, elevated NO levels are known to be pro-inflammatory, partially explaining the tight connection between UVA-induced expression of iNOS along with its photolytic capacity to yield high levels of NO from skin NO derivatives and the development of erythema following unprotected UV exposure [11, 36]. On the other hand, it is important to note that UVA exposure may also lead to photoaging, melanoma (*e.g.*, lentigo maligna) and non-melanoma skin cancers (NMSCs) [37] even though bursts of UVA-induced NO release have shown protective effects against cellular oxidative stresses [38, 39]. Nevertheless, safer light-based approaches to release comparable levels of NO (*e.g.*, red/NIR light) would be preferable.

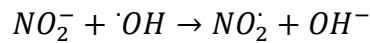
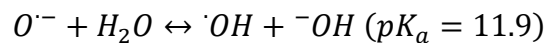
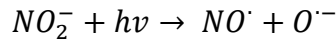
Key Absorption Spectra

It has been acknowledged that UV light liberates NO via photodecomposition of NO derivatives, a process called photolysis, especially photolabile molecules such as nitrite and S-Nitrosothiols (RSNOs).

UVA can release NO radicals from the cutaneous nitrite reservoir. This nitrite photolytic reaction results in the release of NO, and indirectly to the nitrosylation of surrounding biomolecules through the formation of important by-products, like nitrogen dioxide radicals (NO_2^{\bullet}) and N_2O_3 [11].

Compared to NO itself, N₂O₃ is very efficient at nitrosating thiols to RS-NO. It is hypothesized that the formation of N₂O₃ plays a major role in forming RS-NOs (i.e. S-nitroso-albumin), making them more abundant in bloodstream circulation [40]. Besides, photolysis of nitrite is always followed by the release of harmful hydroxyl radicals (*OH*·) [41].

UVA photolysis of Nitrite [11]:



$h\nu$ = light energy

ν stands for frequency (Hz)

h is Plank's constant (6.626×10^{-34} J.s)

Thereby, UVA photons release NO directly by disrupting the Nitrogen-Oxygen bond with a transition state energy of + 87.4 kcal mol⁻¹ [11]. For example, at 320 nm, the radiation energy ($h\nu$) delivered is +89.35 kcal mol⁻¹, easily releasing NO from nitrite stores. Interestingly, the nitrite absorption spectrum falls within the UVA spectral band (Figure 2) [42].

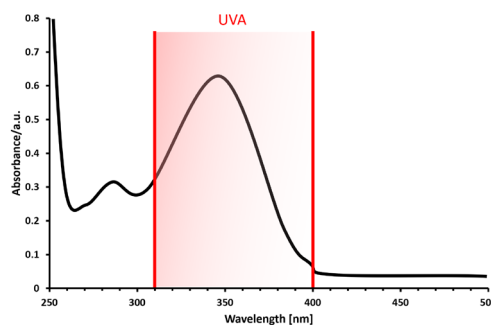


Figure 2. Nitrite absorption peak in the UVA spectra with practically no absorption above 400nm.

As for S-nitrosothiols (RS-NOs), photodecomposition occurs primarily between 290nm and 390nm

[43]. It is known that visible light above 500nm can easily reach the reticular dermis, and in this context, induce significant decomposition of RS-NOs needing lower energy levels to release NO [44].

UVA photolysis of RS-NOs is also taking place in human skin, releasing NO radicals. The required experimental transition state energy needed to decompose RS-NOs have been reported to range from +23 kcal mol⁻¹ to +34 kcal mol⁻¹ [19]. As such, UVA (320 nm – 400 nm) is readily capable of releasing NO from thiol compounds with radiation energies ranging from +89.35 kcal mol⁻¹ to +71.48 kcal mol⁻¹.

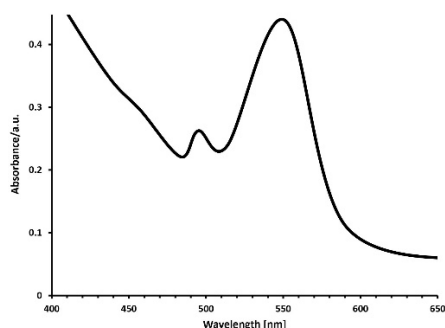


Figure 3. Absorption spectra of a prominent RS-NO, S-nitroso-N-acetylcysteine (SNAC). Note the second absorption peak at 550nm.

Regarding nitrate, although it is physiologically inert, it can be reduced to biologically active nitrite by bacteria in the oral cavity and the gut or reduced by local xanthine oxidoreductases (XOR) [27]. Although its peak absorption (303nm) corresponds to UVB emission spectra [45], UV light (UVB + UVA) has limited ability to photodecompose and release NO. [14, 46]. Paunel *et al.* showed that neither nitrate nor N-nitroso compounds (RN-NO) are involved in the non-enzymatic UVA-induced NO release [13]. However, in vitro studies reported nitrate absorption peaks at 630 & 660nm [47], making it theoretically possible for red light to interact with nitrate for NO release.

It is noteworthy to mention that photodecomposition of nitrite yields lower NO release content compared to RS-NO [18]. However, nitrite photodecomposition is more sustained over time. RS-NO photodecomposition results in much higher NO release content since less energy is necessary to decompose RS-NOs. Nonetheless, the reaction is short-lived, and photodecomposition causes a rapid depletion of RS-NOs in the skin (i.e. photobleaching) [13].

Holliman *et al.* measured the response of four isogenic cell types to UVA irradiation (9 J/cm²) by using a NO quantification reagent DAF-FM DA (4-Amino-5-methylamino-2',7'-difluorofluorescein diacetate) [45]. The four tested *in vitro* cell types were: primary human foreskin keratinocytes, human foreskin melanocytes, human microvascular endothelial cells and human foreskin fibroblasts. They demonstrated that keratinocytes and endothelial cells generated the most significant amount of NO. The higher concentration of RS-NOs within keratinocytes could explain the significant NO response obtained and their proximity to the skin surface. Although melanocytes and fibroblasts showed smaller increases, all cell types released NO. Multiple cell types may release NO *in vitro* following UVA exposure, especially when penetration depth is not restrictive. However, in tissues, cells are located at different depths, especially dermal endothelial cells and fibroblasts. Therefore, visible and NIR photons are better positioned to penetrate and reach them more readily than UV or blue light photons.

Holliman's group also showed that other photoreactions might take place when using visible spectrum photons. They report almost no NO release (% fluorescence) following the irradiation of an aqueous nitrite solution with longer wavelengths (>370nm) using specific bandpass filters applied to a sun simulator [45]. Interestingly, using the same irradiation parameters with wavelengths beyond the UVA spectra, they found a significant NO release by primary human

foreskin keratinocytes, pointing to an alternative NO release mechanism not related to the biologically active form of NO.

Blue light induced NO release

Blue light cutaneous effects are still controversial in the medical literature and appear to be dose dependent. Many studies using blue light with low energy and short exposure time showed promising results in treating some inflammatory skin disorders like psoriasis and atopic dermatitis [48, 49]. The hypothesis outlines the potential of blue wavelengths to reduce proliferation and increase differentiation of keratinocytes along with their potential to downregulate the modulation of immune cells [19]. However, numerous studies reported that by using longer exposure time combined with high-energy (i.e. intensity), blue light may increase the amount of DNA damage [50, 51], cell and tissue death [52], skin hyperpigmentation [53], skin barrier damage [53, 54], premature photoaging [51, 55, 56], and carcinogenesis [50, 51].

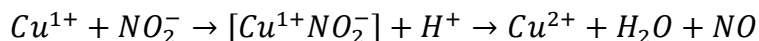
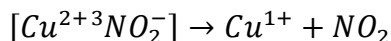
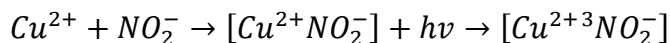
Blue light irradiation modulates cellular behavior by generating ROS and NO bursts. When they both rise by further blue light exposure, skin cells undergo apoptosis [19]. Accordingly, many studies have shown that blue light decreases proliferation and inhibits cellular growth [57-59] possibly due to the absorption of blue photons by porphyrin-containing enzymes and flavins, resulting in the production of ROS bursts [60, 61]. The enzymatic-induced NO release following blue light exposure seems possible via the absorption capacity of flavins needed as cofactors for NOS catalytic activities. Yet, this assumption has only been mentioned in one study [62].

Some work has been done using blue light capable of releasing photolabile NO non-enzymatically [18] the same way ultraviolet does [30]. As mentioned above, the energy needed to decompose RS-NO is relatively low ranging from +23 kcal mol⁻¹ to +34 kcal mol⁻¹. Accordingly, blue light (400

nm – 500 nm) radiation energies, covering +71.48 kcal mol⁻¹ to +57.18 kcal mol⁻¹, can easily photodecompose RS-NO molecules.

As for nitrite, the energy needed to decompose the N-O covalent bond is too high for blue light. Oplander *et al.* found that blue light-induced photodecomposition of nitrite needs the presence of cupric ion (Cu²⁺) and is highly dependent on the reduction of the cupric ion to the cuprous form (Cu¹⁺) [18]. Briefly, copper salts and blue light catalyze the spin-forbidden formation of the intermediate triplet-nitrite (³NO₂⁻), which reduces the Cu²⁺ into Cu¹⁺ via the unpaired-excited electron. Cu¹⁺ will then catalyze the formation of NO via a nitrite molecule, and then water and cupric ion will be released as by-products [19].

Blue light photolysis of nitrite [19]:



In biological environments, copper ions are soluble and mostly bound to specific proteins, like ceruloplasmin and albumin, or other copper-bound proteins [63]. Surprisingly, upon blue light absorption, copper-bound proteins lose their catalytic sites and cannot function properly [19]. As such, it is improbable that blue light-related photodecomposition of nitrite plays an important role in human skin [11]. However, there are relatively high concentrations of nitrite and free copper at the skin surface (12 μM and 10 μM respectively) [11]. Blue light might then decompose nitrite at the apical skin surface.

The resulting NO release following non-enzymatic photolysis (Figure 5) is sufficient to induce a significant increase in local blood flow through vasodilatation or even reduce systemic blood

pressure [64]. Thus, regarding the potency for intracutaneous NO generation from RSNOs, blue light is comparable to UVA-induced effects. These findings reveal the impact and relevance of visible, notably blue light, as an environmental parameter with therapeutic potential for local or systemic hemodynamic disorders. Still, blue-light-induced NO formation from nitrite has different mechanisms compared to UVA-induced nitrite decomposition [16].

Nonetheless, as mentioned above, blue light may induce undesirable long-term cutaneous side effects such as hyperpigmentation [65] and photoaging [66], which is probably due to blue light's proximity to ionizing wavelengths in the UVA spectrum. It is difficult to set a limit at 400 nm securing the skin from ionizing hazards. Several authors now use blue light at 455 nm further away from this borderline to avoid potential overlapping effects and still generate comparable beneficial effects [11, 67, 68].

Red/NIR light therapy: New contenders

Visible light represents approximately 50% of the sun's rays reaching the earth's surface. Other visible light sources are lasers, LEDs and flash lamps [69]. As part of visible light, red light is by far the most commonly used part of the spectrum, especially in light-based low-intensity skin applications with known beneficial effects [70].

On the other hand, a recent review article on the cutaneous effects of visible light reports hyperpigmentation and erythema as potential side effects following exposure to red light [71]. In these studies, very high doses (fluences) (unrealistic environmental solar conditions) were used to treat skin fibrosis [72, 73]. Apart from photodermatoses caused or exacerbated by visible light (solar urticaria, cutaneous porphyrias, and less commonly polymorphous light eruption and chronic actinic dermatitis) [69] red light has an impressive safety profile in PBM [74].

Infrared light (760 nm - 1 mm) constitutes approximately 45% of the solar radiation reaching the ground at sea level [75]. Shortest wavelength near-infrared photons (NIR or IR-A: 760-1400nm) can penetrate the epidermis, dermis and subcutaneous tissue with numerous biological effects [75]. NIR use to have a bad reputation based on past studies using high-intensity artificial light sources (above the solar IR-A irradiance threshold) at high doses leading to detrimental effects (i.e. upregulation of matrix metalloproteinase-1) [76-85]. Although deleterious effects may occur at higher intensities that do not represent real-life daily sun exposure, mimicking sunlight NIR (at lower intensity: 30-35 mW/cm²) will trigger beneficial cutaneous effects [75, 86-90].

Even if therapeutic benefits of red/NIR light therapy have been demonstrated in multiple studies [86, 87, 91, 92], the underlying molecular mechanisms remain poorly understood. The question is no longer whether low-intensity light has biological effects but how these effects are precisely mediated at cellular and molecular levels [93].

As NO is widely known for its function as an intercellular signalling molecule, the release of NO upon red/NIR light exposure would increase its bioavailability, allowing it to function as a signalling molecule [94].

Research shows that red/NIR light could oxidize nitrosyl hemes (i.e. HbNO, MbNO) and release NO using purified systems and myocardial models. Moreover, it has been suggested that NO intracellular signalling could play a role in the upregulation of Cytochrome C Oxidase (CCO). Upon photon absorption, the oxidized iron of Cytochrome a, passing from ferrous (i.e. Fe²⁺) to ferric (i.e. Fe³⁺) iron, can then accept electrons from Cytochrome C, thus increasing the electron flux through the electron transport chain [95]. Red/NIR light has been proposed to influence the photodissociation of NO from CCO, thereby allowing oxygen to reclaim its binding site on the binuclear center, formed of Cytochrome a₃ and CuB [96], allowing ATP production process to resume [90]. For instance, as part of photobiomodulation therapy for the skin's inflammatory

lesions, CCO oxidized state has two absorption peaks at 660nm and 850nm (Figure 4) corresponding to classical red and NIR PBM wavelengths. However, this intramitochondrial reaction is probably not sufficient to significantly impact cutaneous NO stores [92]. Another explication may be towards the red/NIR capacity to generate bursts of ROS and trigger Ca^{2+} influx in skin cells [97, 98]. Both are molecular events upstream of eNOS and nNOS activation through the modulation of calmodulin [99, 100]. Rizzi *et al.* observed an increase in NO concentration by irradiating human keratinocytes at 980 nm [101]. These NO rises were abrogated by treating these skin cells with the NOS inhibitor L-NMMA, thereby proposing an enzymatic involvement of NIR-induced NO release. They proposed that NIR-induced heating may stabilize nNOS and its cofactors. Consequently, using wavelengths in the red and NIR, other NO release mechanisms must be at play.

The efficacy of Red/NIR light to photodecompose NO derivatives has not been proven so far. By virtue of the Planck's equation (i.e., $E = h\nu$), red light at 660 nm and NIR at 850 nm have radiation energies of +43.32 kcal mol⁻¹ and +33.64 kcal mol⁻¹, respectively. In theory, using these two absorption peaks of CCO, their radiation energies should decompose RS-NOs in the skin. Oplander *et al.* showed that green light was able to photodecompose RS-NOs at the same magnitude as blue light [18]. However, many-fold higher irradiances were needed to achieve it. Hence, it is conceivable that red and NIR may photodecompose RS-NOs but not nitrite, needing higher unattainable radiation energy in the red/NIR spectrum. Further investigation is needed to elucidate the true capabilities of red/NIR wavelengths.

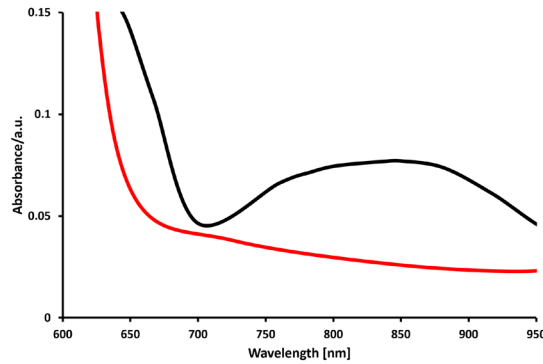


Figure 4. Absorption spectra of Cytochrome C oxidase in the oxidized state (Black) and reduced state (Red) in the visible and near-infrared spectra [102]. It shows higher peaks in the red and NIR at 670 nm and 850 nm, respectively. For instance, at 850 nm, oxidized Cytochrome C oxidase shows ~8% of absorbance compared to ~3 % for its reduced state.

Lately, red and near-infrared wavelengths have been reported to release NO from human skin [25, 101]. Although the mechanism of action is still unknown, it could be much like UV and blue light photolysis of RS-NOs in the skin to free NO into the systemic blood circulation. Another plausible explanation is that epidermal/dermal NO would be released as a result of heat. Accordingly, a temperature-dependent increase in enzymatic activity via NOS would trigger inside-out heating upon the absorption of NIR photons by water in the dermis (figure 5). Temperature rises can actually modulate NO metabolism in the skin. The explanation relies upon heat shock protein 90 (HSP90) that is thermally regulated. HSP90 exerts an allosteric modulation on NOS isozymes by promoting the binding of their cofactors and enhancing their affinity for calcium (for nNOS & eNOS) [103]. Also, HSP90 has shown the capacity to neutralize the NOS isozymes' proteolytic degradation [104].

The non-ionizing safety profile of red and NIR wavelengths makes them logical alternatives to UVA (photoaging and skin cancers) and blue light (persistent hyperpigmentation and photoaging) for NO release skin applications.

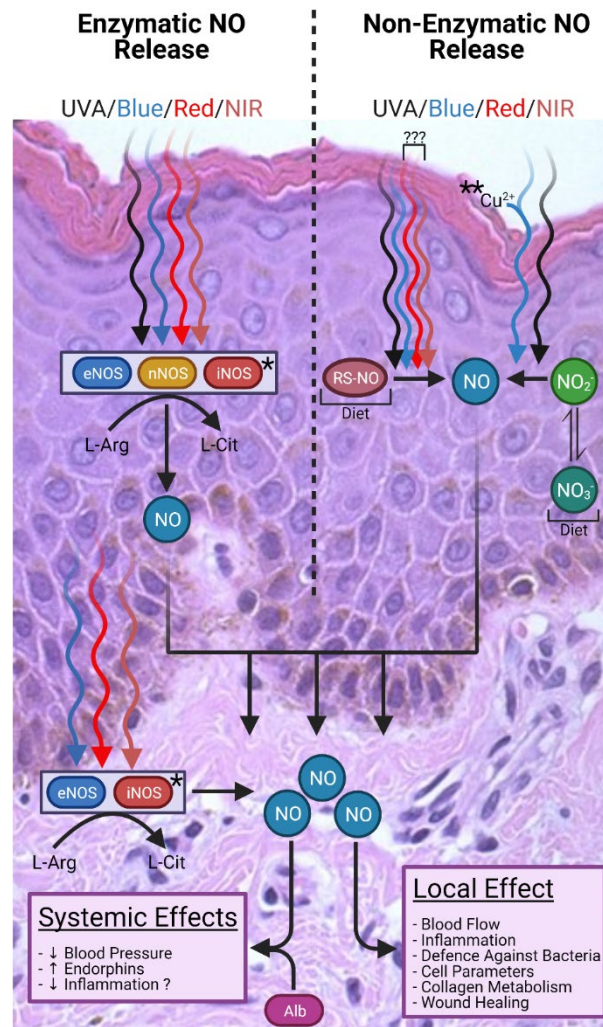


Figure 5. Summary of proposed NO metabolism in the skin with enzymatic and non-enzymatic (photolytic) pathways occurring concomitantly, leading to local and systemic effects. The epidermal activity of NOS enzymes mainly involves eNOS and nNOS. Whereas dermal NOS activities essentially concern eNOS alone, except for mast cells that slightly express nNOS. *In specific conditions, iNOS activation is induced in both epidermal and dermal cells, but it is not constantly expressed compared to nNOS and eNOS. ** Blue light-induced photodecomposition of

nitrite is most likely taking place only at the surface of the skin (i.e., stratum corneum), where there is free copper and a relatively high concentration of nitrite. Albumin (Alb) is proposed as a transporter of very potent NO radicals throughout the body for systemic effects. Red and NIR-related photodecomposition of RS-NOs has not been proven yet but is plausible. Note that nitroso compound (NO_3^- , NO_2^- , and RS-NO) interactions can occur in the following skin cells: keratinocytes, melanocytes, fibroblasts, Langerhans cells, endothelial cells, immunocompetent cells and smooth muscle cells. eNOS: endothelial Nitric Oxide Synthase, nNOS: neuronal Nitric Oxide Synthase, iNOS: inducible Nitric Oxide Synthase, L-Arg: L-Arginine, L-Cit: L-Citrulline, Temp.: Temperature, NO: Nitric Oxide, NO_3^- : Nitrate, NO_2^- : Nitrite, RS-NO: S-Nitrosothiols, and Alb: Albumin. Figure created with BioRender.com

NO Detection Methods in Tissues

Fluorophores

The first method developed for detecting NO was performed via NOS enzyme activity analysis using immunohistochemical methods. A wide variety of methods have since been developed, including the widely used Griess method that detects nitrite as an indirect measure of NO activity [22]. More recently, advanced techniques that directly detect NO radicals have become available such as electron paramagnetic resonance spin trapping. These complex methods are often suitable for measuring NO in fluids or tissue homogenates. When spatial information is required, bioimaging using indicator fluorophores was demonstrated to be a more suitable approach. Newer diaminofluorescein (DAF) dyes/ fluorophores are not cytotoxic, have better specificity for NO and reportedly detect NO down to nanomolar concentrations. 4,5 Diaminofluorescein diacetate (DAF-2 DA) is the cell-permeable version freely diffusing into cells where it undergoes esterification to

form the mildly fluorescent DAF-2. In the presence of NO and O₂, an internal diazotization reaction causes DAF-2 to form the highly fluorescent fluorophore triazolofluorescein (DAF-2 T). This reaction is specific to NO and does not occur with common species related to NO, such as nitrate, nitrite and common reactive oxygen species [105]. In figure 6, an ex vivo skin section stained with DAF-2A is shown, highlighting the presence of NO predominantly concentrated in the epidermis [21]. It is believed that most cutaneous NO stores are located in the epidermis [10, 14].

Other highly sensitive fluorescence probes for nitric oxide based on boron dipyrromethene chromophore will become potentially useful in the future [106].

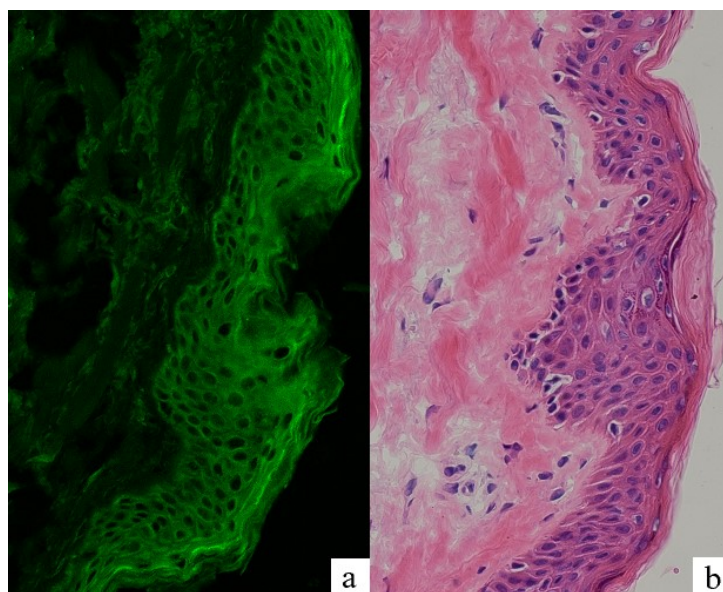


Figure 6. (a) Image of ex vivo skin section treated with the NO detecting fluorophore, DAF-2A mainly concentrated in the epidermis and (b) same skin section stained only with Hematoxylin and Eosin (H&E) [21].

Confocal Microscopy

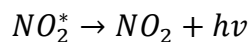
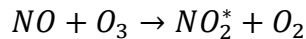
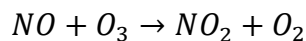
Confocal microscopy offers several advantages over traditional optical microscopy. The two main advantages are the exclusion of background glare and the ability to create optical sections [107]. This is achieved by the difference in the way the image is formed. Conventional optical imaging

creates an image by flooding the entire sample with light, usually using mercury or xenon bulbs. The image is then projected onto an image capture device or viewed directly by the eye. Conversely, confocal scanning microscopy scans a focused beam of light across a small section of the test sample to create an optical section. This method allows imaging of thin layers (the 'Z plane') within a thick section. Also, it reduces the background glare from areas away from the site of interest, as only a small section is illuminated [107]. Lasers generate a focused beam of light and are often used to create better resolution images (laser scanning confocal microscopy). They also allow the choice of an accurate range of wavelengths, which has led to the development of specific fluorophores [105].

Chemiluminescence

The release of NO in aqueous nitrite solutions visible LED irradiation can be investigated at skin-relevant pH values (pH 5.5). According to the Kolbe electrolytic method, the NO developing in the solution is flushed out with inert gas and determined with a chemiluminescence detector (CLD). An increase in BSO (buthionine sulfoximine) nitrosation is an indication that the light source used decomposes nitrite photolytically. A decrease of protein nitrosation in the absence of nitrite during exposure thus indicates that the wavelength used is able to release the NO locked in the nitroso BSA (bovine serum albumin). The nitrosation of proteins is then determined through chemiluminescence detection [57].

The release of vasoactive NO can be measured at the time of release. NO reacts quickly with ozone (O_3) to form either nitrogen dioxide (NO_2) or nitrogen dioxide in its excited state (NO_2^*). When NO_2^* decays to the ground state, photons are emitted with electromagnetic radiation ranging from 600 nm to 3000 nm [108]. Therefore, the emitted light is quantified, and this is proportional to the amount of NO in the sample. The overall reaction is known as such [109]:



Usually, CLD is a device that has a cold chamber where the reaction takes place. In this chamber, there is a photomultiplier (PMT) that contains a photosensor, which converts incident photons into an electrical signal. Sometimes the redox reaction releases photons at a very low energetic level, so PMT needs to be kept at -20 °C to optimize the photodetection efficacy. O₃ is directly injected into this cold chamber to react with the NO found in the sample. NO₂ and O₂ are immediately extracted via a small vacuum, thereby letting the remaining NO in the sample be detected without interacting with these former by-products. PMT electrical signal is transformed into a ratio concentration via a calibration table, such as part-per-million (PPM) or part-per-billion (PPB) units. In most NO-detection experiments using CLD, ambient air, which contains O₂ and derivative oxygen molecules, is extracted from the sample and replaced by argon gas. None of the NO content in the sample can react with oxygen molecules until it reaches the cold chamber to be adequately quantified. Therefore, a flowmeter is often utilized to measure the exact concentration of argon that is found in the sample. The argon concentration can then be used along with the concentration ratio given by CLD to provide the exact concentration of NO in the sample. This technique is helpful in a variety of experimental models, including in vivo on patients, in processed tissues, reconstituted skin models and cell lines. Hence, CLD is widely used to detect NO for its simplicity, exactitude, and extensive application range.

Griess Assay

The indirect measurement of nitrogen oxides concentration (i.e. total nitrate and nitrite concentration (NO_x)) is regularly used as an indicator of NO production in biological systems [110]. Griess Reaction was first introduced in 1879 by Dr. Peter Griess [111]. Through the years, it has been used widely in the analysis of numerous biological samples, such as plasma (serum), saliva, CSF, urine, and cell culture media [110].

In this assay, the sample is treated with a diazotizing reagent, like sulfanilamide (SA), in an acidic media where the sample's nitrite content interacts with it to form a transient diazonium salt. Then, this diazonium intermediate reacts with a coupling reagent, like N-naphthyl-ethylenediamine (NED), thereby forming a stable azo compound [110]. Griess assay has high sensitivity and can detect nitrite concentration in a biological sample as low as ~0.5 µM. The absorbance peak of the Griess mixture is at 540 nm, and this is linearly proportional to the nitrite concentration found in the sample [110]. Variations in the technique exist among published Griess assays. For instance, the diazotizing reagent and the coupling reagent are added, either simultaneously or sequentially, to the biological sample. The technique often utilized seems to be the sequential way, in which the sample is mixed with SA initially, followed by the addition of NED. This technique seems to give higher fluorescence of the azo compound chromophore, and thereby more sensitivity to detect NO_x in biological samples [112, 113].

The Relevance of Light-induced NO Release in Human Skin

NO mobilization leads to Local & Systemic effects

Three steps are involved in light-skin interactions to mobilize NO stores. First, light liberates nitric oxide from photo-labile intra-cutaneous NO metabolites. Second, a fraction of the highly mobile NO diffuses towards the outer surface escaping in the ambient atmosphere (detectable by airtight

skin chamber and chemiluminescence) [25]. A different NO fraction diffuses to deeper tissue layers, where it enters the capillary vessels and enhances local levels of RS-NO. These nitrosated species have low molecular weight, like glutathione-S-NO or albumin-S-NO [11]. The third step is the distribution of relatively stable nitroso compounds via the blood circulation, where it may elicit a systemic response such as a measurable decrease in blood pressure [114] and perhaps other effects in distant organs (Figure 7).

NO Local Effects

Several findings indicate that the balance between NO and ROS during UVA exposure determines the cellular fate [115]. The current debate to characterize NO is still open. Intracellular NO concentration seems to depend on the cell's redox potential and NO's resting levels. Therefore, the photolysis of nitrite has a two-sided effect [116]. It combines the beneficial release of cutaneous NO with the harmful production of hydroxide (OH) and nitrogen dioxide (NO₂) radicals. In human skin cells, even supraphysiological high NO concentrations were shown to protect cells from oxidative stress and UVA-induced apoptosis [117]. Indeed, the skin nitrite content and apical acidity provide a favorable environment to foster NO protective effects.

On the other hand, in other cell types (i.e. extra-cutaneous), NO had been shown to promote apoptosis even at "physiological" concentrations [11].

In order to facilitate cell protection and scavenging of OH or NO₂ radicals, the promotion of NO should take place. This can be achieved by exogenously applied NO or antioxidants against UVA/nitrite-induced cell death (radical formation) [118]. In addition, low-intensity visible/NIR light-induced NO enhancement is now possible, as mentioned earlier.

The promotion of wound healing was among the first observed PBM benefits, now substantiated by well-designed controlled human studies. Low-intensity light treatment parameters can be

tailored to account for pathophysiologic responses in the skin corresponding to the type of vulnerable wound at stake [119]. The effect of NO release by PBM wavelengths on local wound healing has been reported with supportive evidence [92].

Wound re-epithelialization is regulated by mediators such as NO. An in vitro study showed a rise in NO production in human keratinocytes using low-intensity NIR (980nm) light that might be directly related to the re-epithelialization process [101]. Another study using a mouse model by Moriyama *et al.* measured iNOS gene expression modulated by several PBM wavelengths (635, 660, 690, and 905 nm) in CW (continuous wave) and pulsing modes. They found that animals younger than 15 weeks showed reduced iNOS expression, while older animals showed a rise in iNOS expression. Light intensity and time course of iNOS expression were found to depend on wavelengths and delivery modes [120].

The next challenge in the field will be to clarify the mechanism of action of other non-ionizing wavelengths (visible and near-infrared) to release NO from the huge S- and N-nitroso compounds epidermal reservoir.

NO Systemic Effects

NO reacts extremely rapidly with surrounding molecules, either proteins, biomolecules, or oxygen species. It has a half-life of a few seconds. Moreover, its diffusion rate is very high at $D \sim 3300 \mu\text{m}^2 \text{ s}^{-1}$ at 37°C [11]. For instance, its diffusion rate is about 1,4-fold higher than O_2 or carbonic oxide (CO) [11]. Hence, it can easily penetrate the cell membranes and reach up to $500 \mu\text{m}$ in tissues. How can NO reach distant organs with systemic effects in the human body if it dissipates rapidly at the site of release? How can it be transported throughout the body?

Oplander *et al.* have conducted some studies to elucidate NO transportation mechanisms [18, 64]. They found that it is primarily RS-NOs that transport NO systemically. Larger concentrations of

RS-NOs were found in the blood plasma following UVA and blue light irradiation, especially S-nitroso-albumin. Albumin composed 50-60% of the human blood plasma [63]. This makes it readily available to be nitrosated by light-induced NO radicals. Albumin is formed of 585 amino acids organized in three homologous domains, each having five or six disulfide bonds. Only its cysteine residue 34 has a free thiol group that can be nitrosated [121]. Like hemoglobin that transports oxygen throughout the body, albumin is now the presumed NO carrier in the blood circulation transporting and releasing NO into vascular networks leading to vasodilation away from the irradiation site [11].

Systemic arterial hypertension is a significant public health issue with several environmental stressors and a much higher risk of cardiovascular complications, including coronary artery disease, heart failure and sudden death [122], even in young adults [123]. Interestingly, mean systolic and diastolic pressures and the prevalence of hypertension vary throughout the world. Many data suggest a linear rise in blood pressure at increasing distances from the equator [124, 125]. Interestingly, epidemiological studies show that lack of sun exposure has a considerable impact in northern countries, considering that a decrease in 10 mmHg of people's blood pressure translates into a fall of 5 % risk in cardiovascular complications [123].

Similarly, blood pressure is higher in winter than in summer [126, 127]. Daylight length and ambient temperature also correlate inversely with BP [128, 129]. Recently, Weller *et al.* showed that in addition to environmental temperature, incident solar UV radiation is associated with lower blood pressure in a large and diverse cohort of chronic hemodialysis patients [124]. Apart from reduced vitamin D stores and increased parathyroid hormone secretion [130] as a possible explanation, there might be another supporting mechanism by which ambient electromagnetic radiation may affect blood pressure. In a seminal experiment (1961), Robert Furchgott *et al.*

showed that light exposure could relax isolated arterial strips of rabbit aorta [131], paving the way to his 1998 Nobel prize explaining the impact of NO on endothelial cells.

Besides, endogenous photo-sensitive NO derivatives may be influenced by dietary nitrate and nitrite intake [132]. Accordingly, dietary nitrate supplementation combined with UV exposure has been shown to increase nitric oxide (NO) metabolites, reduce blood pressure (BP) and enhance exercise performance [28]. Photobiomodulation at 904nm (NIR) alone can also prevent exercise-induced skeletal muscle fatigue in young women in part due to systemic NO release [133].

Other applications using NO release mechanisms are reported in psychiatry and neurology, where the systemic effects of PBM may achieve neurorehabilitation [134]. Likewise, this application could be of great help in dermatology, especially in neurodermatitis and prurigo nodularis, where two components of these psycho-cutaneous diseases (behaviour and skin) are targeted. However, the systemic effects on mood are often subjective and not easy to measure [135].

Lastly, PBM's anti-inflammatory effects are well described and partly explained by the release of biologically active molecules like NO [87]. The effects of NO on biological tissues are complex and multifaceted [136]. Upon systemic release following large surface body exposure via light-emitting diode (LED) beds, NO can probably induce multiple site-specific beneficial effects to distant organs (figure 7), including the modulation of inflammation in remote unexposed areas. Such systemic impacts will possibly lead to anti-inflammatory applications such as arthritis.

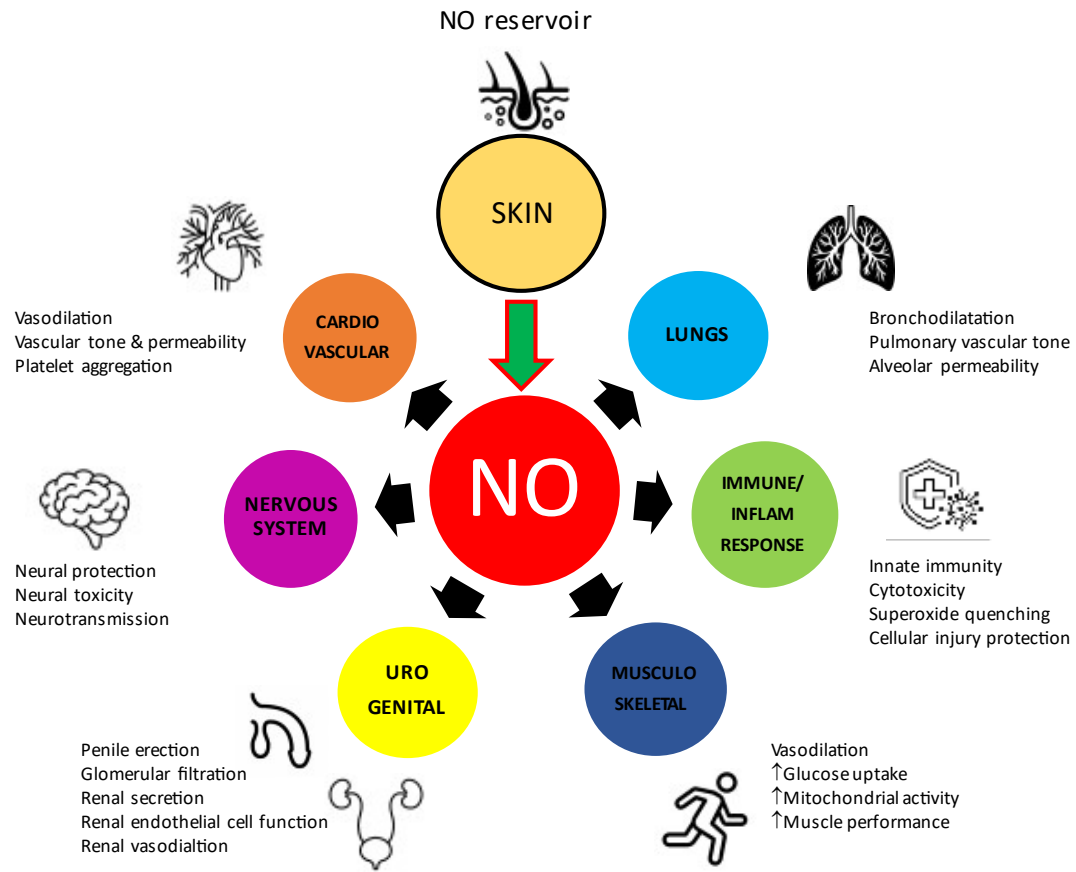


Figure 7. NO release from the skin to remote body organs may trigger site-specific beneficial effects. NO plays a crucial role as a vasodilator, bronchodilator, and immune/inflammatory mediator. Note that skin NO content is 6x higher than in blood circulation.

Hypothesis and Aims

We hypothesized that NIR and red wavelengths are capable of releasing NO in the skin, either enzymatically or non-enzymatically. The aim of this work was to measure the NO concentration in an *ex-vivo* human skin model following exposure to UVA (365 nm), red (660 nm), and NIR (850 nm) light exposures. The secondary aim of the study was to evaluate the enzymatic vs non-enzymatic magnitudes by assessing the involvement of NOSs using a non-selective NOS inhibitor

L-NMMA and a NO scavenger carboxyl-PTIO (CPTIO). NO concentrations were measured indirectly for each condition using a colorimetric Griess assay method.

Methods

Table of Materials

LED – Diodes; 365 nm (LZ130UV0R0000), 660 nm (LZ100R2020000), 850 nm (LZ100R6020000)	LED Engine inc.
<i>Custom</i> Reaction chamber – Aluminum Block. Multipurpose 6061 Aluminum Hex Bar	McMaster-Carr, Illinois, USA
Water Chiller – Solid state Recirculating Chiller	ThermoTek inc., Flower Mound, Texas, USA
<i>Custom</i> LED Controller board	Digi-key Electronics, Minnesota, USA
Phosphate Buffered Saline	Sigma-Aldrich, St-Louis, Missouri, USA
Falcon 50 mL conical centrifuge tubes. Corning Life Sciences (C352070)	Thermo Fisher Scientific, Massachusetts, USA
Tissue-Tearor Homogenizer (Model 985370-14)	Biospec Products, Oklahoma, USA
TG18.5(TG1850-WS) Tabletop High Speed Centrifuge, LuXiangyi Brand	AliExpress, Online shopping site
Sample bottles with plastic snap cap (HDPE sample bottles). DWK Life Sciences Wheaton.	Thermo Fisher Scientific, Massachusetts, USA

Griess reaction assay Kit – QuantiChrom NO assay kit	Avantor, VWR company, Mississauga, Ontario, Canada
Zinc sulfate solution 0.3 N	Sigma-Aldrich, St-Louis, Missouri, USA
Sodium Hydroxide, pellets, $\geq 98\%$	Sigma-Aldrich, St-Louis, Missouri, USA
Amicon Ultra-0.5 Centrifugal Filter Unit, 24-pack	Thermo Fisher Scientific, Massachusetts, USA
Denville Vortexer 59A	Thermo Fisher Scientific, Massachusetts, USA
Spectrophotometer, UV765 series UV-Vis	AliExpress, Online shopping site
Fisherbrand Polygon Stir Bar (20 X 8 mm)	Thermo Fisher Scientific, Massachusetts, USA
Fisher, Magnetic stirrer, Cat No. 14-511-1	Thermo Fisher Scientific, Massachusetts, USA
Small volume cuvette, Eppendorf, UVette cuvettes (50 to 2000 μL)	Thermo Fisher Scientific, Massachusetts, USA
Alfa Aesar Carboxy-PTIO potassium salt, 98+%	Thermo Fisher Scientific, Massachusetts, USA
NG-Methyl-L-arginine acetate salt, $\geq 98.0\%$	Sigma-Aldrich, St-Louis, Missouri, USA
Sodium nitrite (NaNO_2) ReagentPlus, $\geq 99.0\%$	Sigma-Aldrich, St-Louis, Missouri, USA
Fisherbrand Premium Microcentrifuge Tubes: 1.5mL	Thermo Fisher Scientific, Massachusetts, USA
Water (HPLC), Fisher Chemical (W5-4), low in nitrite and nitrate.	Thermo Fisher Scientific, Massachusetts, USA
Thermo Scientific, Long-Term Storage Cryogenic Tubes, 2 mL (50000020)	Thermo Fisher Scientific, Massachusetts, USA

VWR® Mini Centrifuges (76269-064)	Avantor, VWR company, Mississauga, Ontario, Canada
Microsoft Excel, 2021 Computer Software	Microsoft, Washington, USA
GraphPad Prism 9.1.0 Computer Software	GraphPad Software, California, USA
BioRender, 2021 Online Application	BioRender, Toronto, Ontario, Canada

Table 1. List of materials utilized to run the following protocol.

Experimental design

This experiment was designed to assess the capacity of red and NIR to release NO in human skin tissue. Therefore, we used a Griess reaction assay to measure nitrite levels on human skin homogenate following light exposures at 365 nm, 660 nm, and 850 nm. These three conditions were compared to a sham group (i.e. no irradiation). Moreover, the involvement of NOS was evaluated by treating our human skin homogenate samples with non-selective NOS inhibitor L-NMMA. As a negative control, the Griess mixture was tested by using the NO scavenger carboxy-PTIO (C-PTIO). The experiment was divided as follows:

1. Light treatment vs Sham experiment
2. L-NMMA control experiment
3. C-PTIO control experiment

Each section had a common protocol and was sub-divided into five steps, as follow:

1. Skin homogenate preparation
2. Skin homogenate incubation
3. Skin homogenate treatment
4. Griess reaction assay
5. Data analysis

Each section of this experiment was performed over five days, steps 1 to 3 in the first three days, and then the remaining steps (4 and 5) were completed in the last two days (day 4 and day 5). The skin biopsies were coming from McGill Biobank at McGill University Health Centre (November 2020). In total, there were 12 skin biopsies from eight different human donors. Skin samples were all weighing approximately 1 gram, eventually yielding 30 mL of skin homogenate at 3% weight per volume (% W/V) per sample.

Skin homogenate preparation

Full-thickness human skin was obtained flash-frozen from McGill Biobank. Samples were thawed for 5 minutes, and for each sample, 0.9 gram was extracted and added to a 50 mL falcon tube. Then, 30 mL of phosphate-buffered saline (PBS) was added and ground up with the tissue grinder. After spun it down at 560 g for 1 minute, 30 mL of the supernatant was collected and separated equally in three 15 mL falcon tubes, each containing 10 mL of skin homogenate sample.

Skin homogenate incubation

Incubation protocols were needed only for both L-NMMA and C-PTIO experiments. All incubation procedures were performed at 22 °C. Details of the experiments are illustrated in figure 8, as follow:

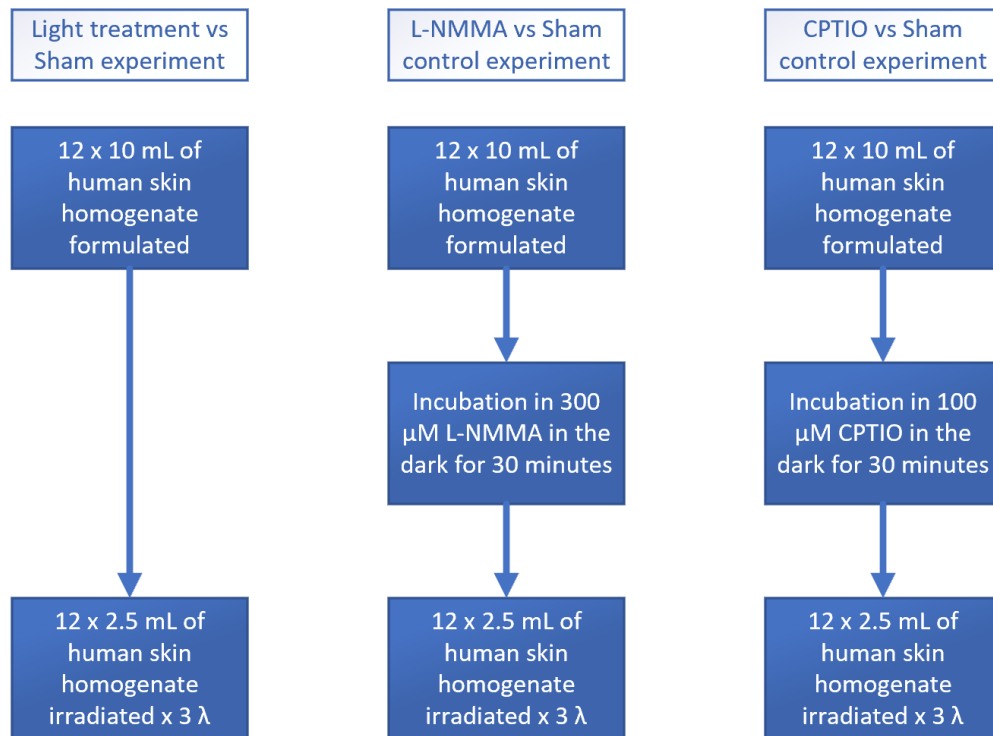


Figure 8. Human skin homogenate preparation and incubation protocol.

Skin homogenate treatment

For each treatment, 2.5 mL of skin homogenate was added to a sample bottle with a stir bar in it. Then, the sample bottle was inserted into a custom reaction chamber.

This reaction chamber was designed and built in the lab where the experiment was conducted. It was designed to enclose the skin homogenate in the dark, letting only a small opening for exposure to the tested light source (UVA, red and NIR). Also, it kept the reaction chamber at a constant temperature during light exposure. The reaction chamber was built using a computer-assisted (from CAD drawings) CNC machine milling a solid aluminum block.

Internal flow channels were drilled around the sample bottle (glass reaction vessel in purple), forming a water cooling heatsink block (figure 9 green #2).

Hence, in and out connectors of the reaction chamber were connected to a solid-state chiller and kept at a given temperature during each light treatment. The design of this reaction chamber is shown below in figure 9.

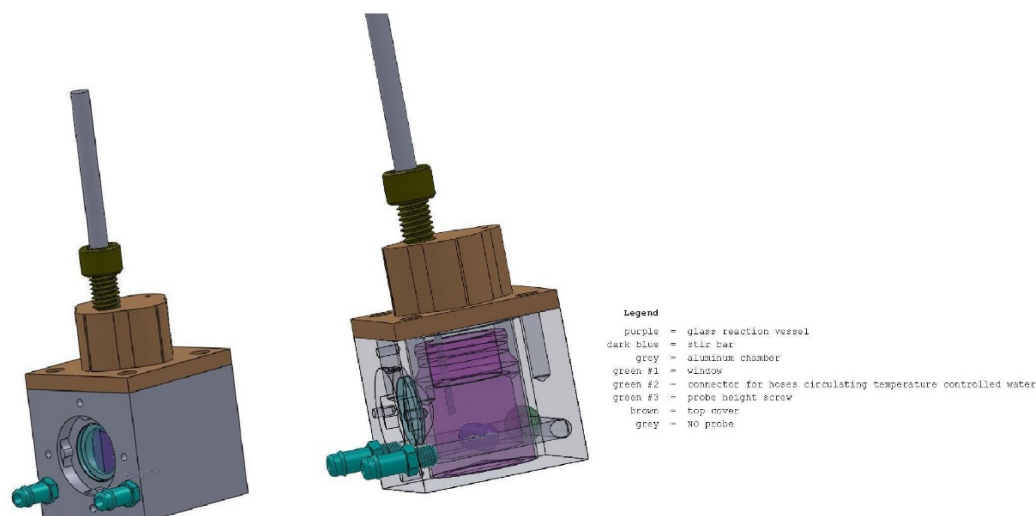


Figure 9. CAD drawing of the reaction chamber

The role of the chiller is crucial since skin homogenate temperature must be kept constant during light exposure. Indeed, the light source itself may increase the temperature of skin samples during, or following exposure via the absorption of light by chromophores like water in the skin homogenate. Moreover, since the NOS metabolism is greatly influenced by heat, it was imperative to control the temperature. A small light module with three diodes (three wavelengths; 365, 660, 850nm) was designed to perfectly fit the small window (figure 10) of the reaction chamber to directly irradiate the skin homogenate placed inside the glass reaction vessel (transparent glass container) (figure 10). The light module was connected to a custom-built LED controller to set light irradiation parameters, such as irradiance and fluence. The reaction chamber was connected to a solid-state chiller (set at 22 °C) and dropped on a magnetic stirrer plate set at a low speed (speed 3). Skin samples were then irradiated with their respective tested wavelength (365nm or 660 nm or 850 nm) at irradiance 50 mW/cm² for 600 seconds, for a total fluence of 30 J/cm² delivered.

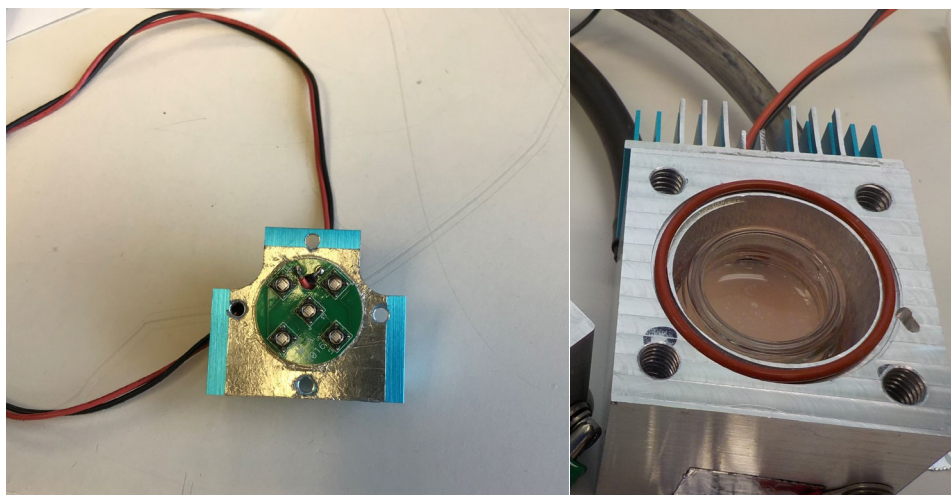


Figure 10. Pictures of the light module (Left) and a skin homogenate placed in the custom reaction chamber (right).

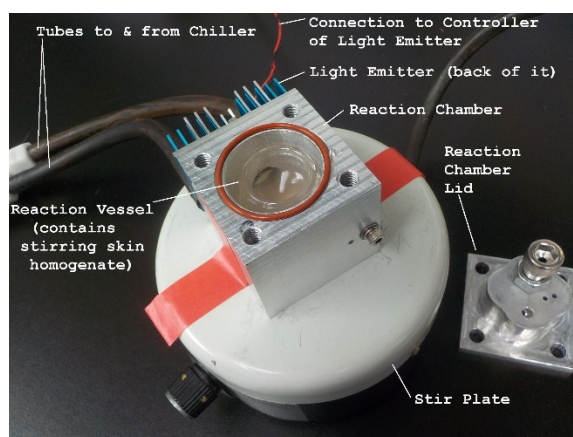


Figure 11. Custom Designed & Built Reaction Chamber. In the irradiation experiments, skin homogenate is kept stirring at 22°C while it is irradiated.

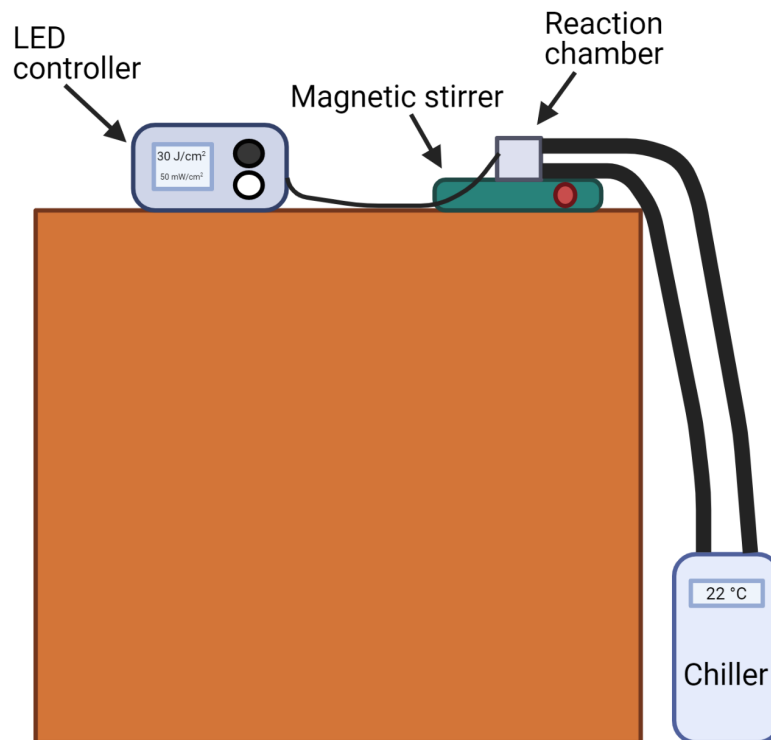


Figure 12. Schematic of the experimental setup of the skin homogenate light treatment. This figure was sketched on Biorender.com

Immediately after the treatment, 1.8 mL of the treated sample was flash-frozen in a 2 mL cryotube for further analysis.

Griess reaction assay

Flash-frozen samples were thawed and transferred into a 2 mL microfuge tube. They were then centrifuged at 10 000 g for 5 minutes, and the supernatant was kept for the following procedures.

First, the sample supernatant was deproteinized to avoid a low fluorescence rate from the Griess reaction due to the high content of protein and high turbidity of the sample. The Deproteinization step is essential in the Griess analysis method for skin homogenate samples [110]. Nitrite content

found in our samples can be easily converted to NO and nitrogen dioxides under acid conditions; therefore, acid protein precipitation methods were avoided.

900 μL of the supernatant sample was added to a 1.5 mL microfuge tube. Afterwards, 48 μL of zinc sulfate (ZnSO_4) was added to the sample microfuge tube and vortexed. Then, 48 μL of sodium hydroxide (NaOH) was mixed into the sample and vortexed. Finally, the microfuge tube was centrifuged at 12 000 g for 10 minutes, and 500 μL of the supernatant was filtered with the Amicon Ultra-0.5 centrifugal filter kit following the manufacturer guidelines. Between 300 and 400 μL of the filtrate was obtained following the deproteinization, which was divided into three 1.5 mL microfuge tubes at 100 μL each.

After the deproteinization, the Griess reaction assay was performed on each sample. Following the manufacturer guidelines (Quanticom NO assay kit), standards and the master reaction mixture, which contains the diazotizing and coupling agent, were prepared. Then, 200 μL of the master mix was added to each sample and standard. Subsequently, they were vortexed and incubated at room temperature for 150 minutes in the dark. Afterwards, the tubes were spun down, and 300 μL of each microfuge tube was added to a separate Eppendorf cuvette. Finally, each cuvette was inserted into the spectrophotometer to measure their optical density at 540 nm (OD_{540}).

Data analysis

OD_{540} values of the standards were used to make a standard curve. This curve was then utilized to measure the estimated concentration of nitrite in each human skin homogenate sample. This compilation was executed in Microsoft Excel 2021. It is worth mentioning that all the OD_{540} values of our samples were inflated by a factor of 1.107 (i.e. 96 $\mu\text{L}/900 \mu\text{L}$). This inflation was necessary to accommodate the dilution previously done with ZnSO_4 and NaOH to deproteinize the skin homogenate supernatant samples.

The nitrite concentration values were then compiled in the GraphPad Prism 9 software. A paired t-test was calculated to compare each condition to their respective sham group. Also, a 95% confidence interval was computed for each condition. A statistical comparison between the L-NMMA and the irradiated sham group was also assessed, this time using an unpaired t-test with the Welch correction. The same statistical test was performed to compare the C-PTIO and the irradiated sham group. Since the data provided are continuous and their means represent the center of their distribution, added to the fact that parametric tests have more statistical power for smaller distribution, only parametric tests were used in this work. Graphs provided for the Results section were all made using the GraphPad Prism 9 software.

Results

The three main experiments are discussed separately in this section. Also, the last section discusses the statistical comparisons made between the three experiments.

Results 1 – Light treatment vs. Sham experiment

The concentration of nitrite detected in each sample was compared between samples taken before the light irradiation (i.e. Sham group) and their respective samples taken after the light treatment. Three wavelengths were assessed in their capacity to release NO in a human skin homogenate model. These wavelengths were UVA (365 nm), red (660 nm), and NIR (850 nm). The fluence and irradiance were identical for each wavelength and as follows, 30 J/cm² and 50 mW/cm², respectively.

Data Comparison	Paired t-test
UVA (365nm) 30 J/cm ² vs. Sham 0 J/cm ²	0.0001 (***)
Red (660nm) 30 J/cm ² vs. Sham 0 J/cm ²	<0.0001 (****)
NIR (850) 30 J/cm ² vs. Sham 0 J/cm ²	<0.0001 (****)

Graph 1. Irradiated vs. Sham Data

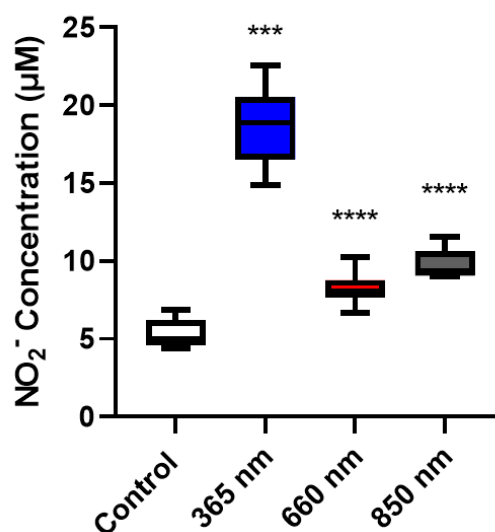


Table 2. Statistical analysis of Irradiated vs. Sham experiment

Mean concentrations of nitrite were calculated for each condition and displayed on graph 1. A paired t-test was performed to compare each condition to their paired sham group. Our results show that red (660 nm) and NIR (850 nm) are capable of releasing NO in the skin compared to sham groups (i.e. no irradiation) with statistical significance. Moreover, as expected, our benchmark UVA (365nm) light exposure shows the greatest mean concentration of nitrite at $18.69 \pm 2.75 \mu\text{M}$ compared to the two other tested wavelengths.

Results 2 – L-NMMA control experiment

The effect of adding the non-selective NOS inhibitor L-NMMA to the human skin homogenate was assessed in this experiment. 300 μM of L-NMMA was added to each skin homogenate before irradiation. As in the first experiment, the same three wavelengths (365, 660, and 850nm) were evaluated using the same fluence and irradiance. Data are illustrated in graph 2 below.

Data Comparison	Paired t-test
UVA (365nm) 30 J/cm ² vs. Sham 0 J/cm ²	<0.0001 (****)
Red (660nm) 30 J/cm ² vs. Sham 0 J/cm ²	0.0046 (**)
NIR (850) 30 J/cm ² vs. Sham 0 J/cm ²	0.0056 (**)

Graph 2. L-NMMA vs. Sham Data

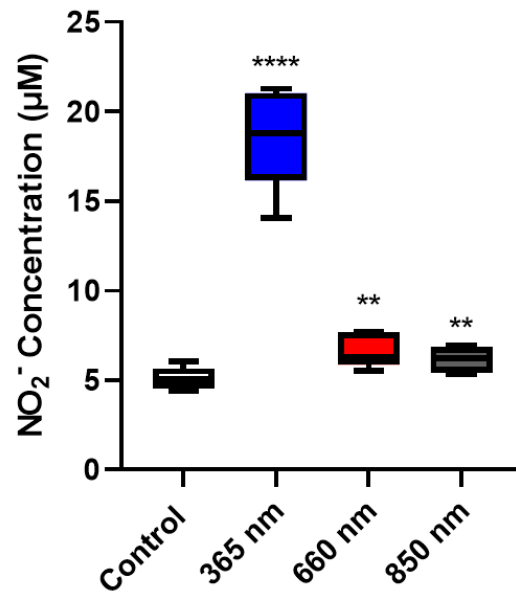


Table 3. Statistical analysis of L-NMMA control experiment

Mean concentrations of nitrite with 300 μM of L-NMMA was calculated for each tested wavelength and compared to their respective sham group. Our data show that L-NMMA does not completely block the release of NO in our human skin homogenate model. Each wavelength mean concentration of nitrite was statistically significant compared to sham groups. Again, UVA (365 nm) demonstrates the greatest potential to release NO non-enzymatically with $18.45 \pm 2.92 \mu\text{M}$ of nitrite and a p-value of <0.0001.

Results 3 – C-PTIO control experiment

The effect of the selective NO scavenger C-PTIO was evaluated in this control experiment. The human skin homogenate was incubated with 100 μM for 30 minutes in the dark. Here, the same wavelengths previously used were tested with similar light parameters (fluence and irradiance, at 30 J/cm^2 and 50 mW/cm^2 , respectively). Results are shown in graph 3 below.

Data Comparison	Paired t-test
UVA (365nm) 30 J/cm^2 vs. Sham 0 J/cm^2	0.0005 (***)
Red (660nm) 30 J/cm^2 vs. Sham 0 J/cm^2	0.5511
NIR (850) 30 J/cm^2 vs. Sham 0 J/cm^2	0.1498

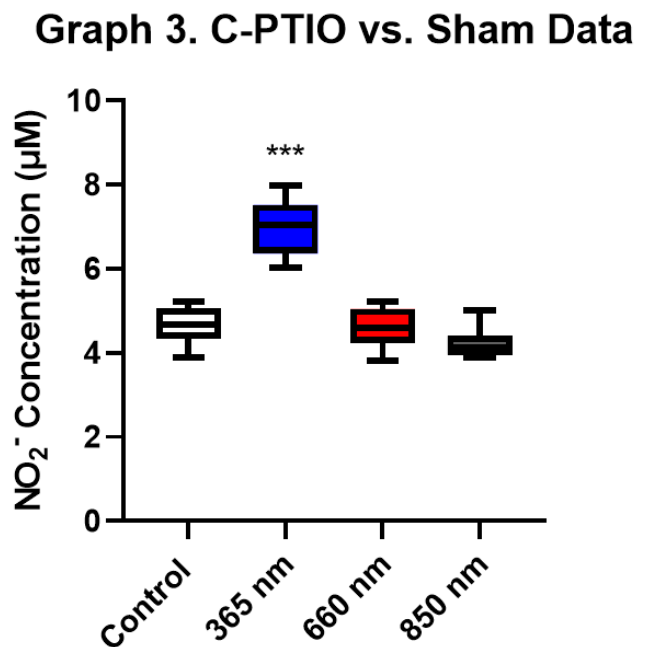


Table 4. Statistical analysis of C-PTIO control experiment

Mean concentrations of nitrite were determined for each wavelength and compared to their respective sham group. Negative control C-PTIO decreased greatly red- and NIR- related NO release. Indeed, following C-PTIO incubation, red and NIR show no statistical difference compared to their sham group with p-values of 0.55 and 0.15, respectively. Surprisingly, UVA (365 nm) is the only wavelength showing a statistical significance in releasing NO even with the selective NO

scavenger C-PTIO ($6.99 \pm 1.12 \mu\text{M}$ and a p-value of 0.0005), although at much lower levels than the two former experiments.

Combined comparisons

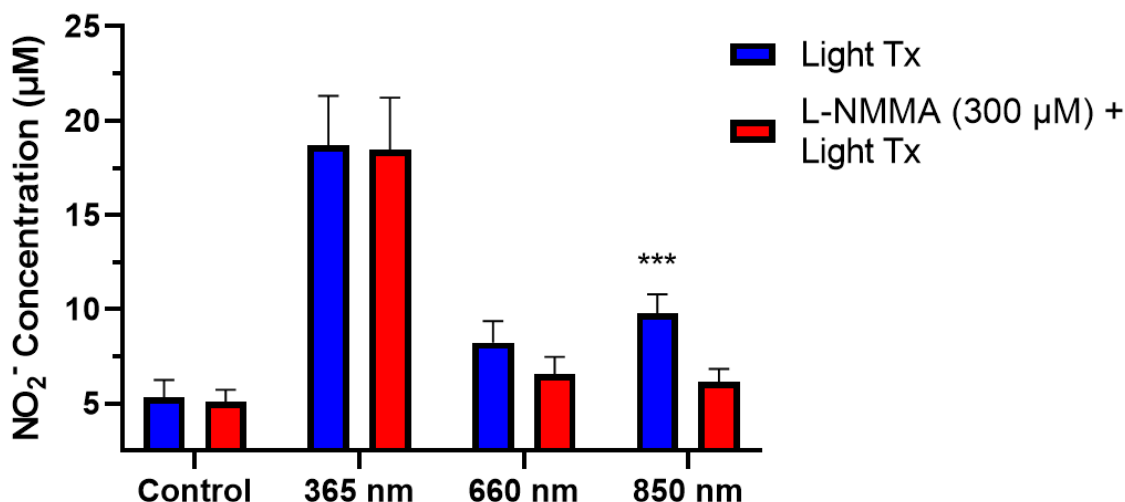
Experiment 1 (only light treatment) vs. Experiment 2 (L-NMMA)

By using GraphPad Prism 9, a statistical comparison was computed between two types of irradiated samples; not incubated with any molecule (experiment #1) and the ones incubated with the non-selective NOS inhibitor L-NMMA (experiment #2). For this application, an unpaired t-test with Welch correction was used to assess the statistical significance of this comparison. Data are illustrated in graph 4.

Data Comparison	Unpaired t-test adjusted with Welch approach
UVA (365nm) 30 J/cm ² vs. Sham 0 J/cm ²	0.877520
Red (660nm) 30 J/cm ² vs. Sham 0 J/cm ²	0.060344
NIR (850) 30 J/cm ² vs. Sham 0 J/cm ²	0.000230 (***)

Table 5. Statistical analysis of Experiment 1 vs. Experiment 2 comparison

Graph 4. Experiment 1 vs. Experiment 2



The difference in the mean nitrite concentration between the blockage of NOSs and their respective L-NMMA non-treated group is only statistically significant using NIR (850 nm) light with a mean difference of 3.608 μM of nitrite and a p-value of 0.0002. Other wavelengths show no statistical significance when using L-NMMA.

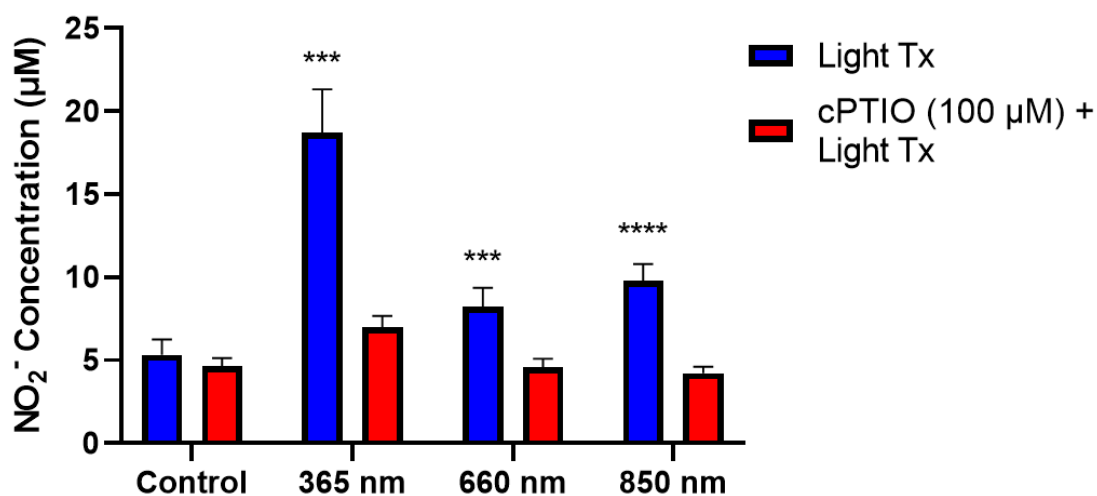
Experiment 1 (only light treatment) vs. Experiment 3 (C-PTIO)

Another comparison was made between two other irradiated samples, such as samples incubated with selective NO scavenger C-PTIO (Experiment #3) and the one irradiated by light alone (Experiment #1). Like the previous comparison, an unpaired t-test with the Welch correction was executed to compare them. Data of this assessment are displayed on graph 5 below.

Data Comparison	Unpaired t-test adjusted with Welch approach
UVA (365nm) 30 J/cm ² vs. Sham 0 J/cm ²	0.000178 (***)
Red (660nm) 30 J/cm ² vs. Sham 0 J/cm ²	0.000440 (***)
NIR (850) 30 J/cm ² vs. Sham 0 J/cm ²	0.000035 (****)

Table 6. Statistical analysis of Experiment 1 vs. Experiment 3 comparison

Graph 5. Experiment 1 vs. Experiment 3



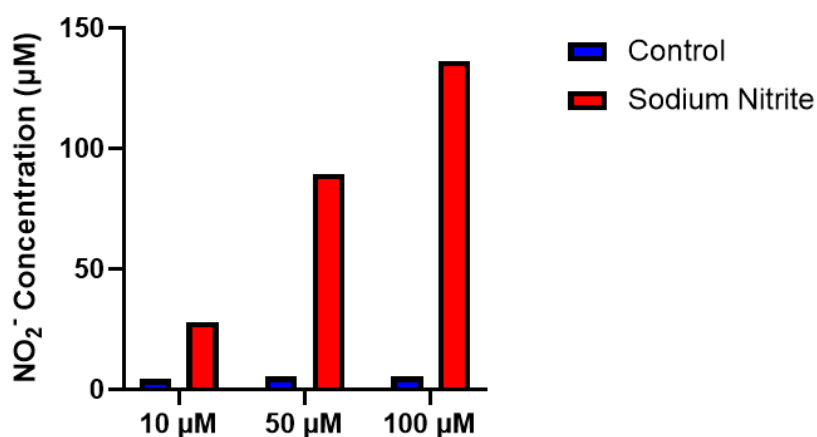
The mean differences between the CPTIO human skin homogenate samples (Experiment 3) and the only irradiated samples (Experiment 1) were all statistically significant. UVA (365 nm) shows the highest mean difference with 11.70 µM of nitrite and an adjusted p-value of 0.000178. At the

same time, NIR (850 nm) displays the greatest statistical significance with an adjusted p-value of 0.000035.

Discussion

The Griess reaction is a fast and simple colorimetric assay for nitrite. It proved to be a reliable quantitative NO measurement method in ex vivo skin homogenate exposed to various PBM light sources in the UV / red / NIR spectra. However, it has limitations that were considered while designing the protocol for these experiments. Griess reaction assay is an indirect measuring method of NO by measuring nitrite ions in a biological sample. Since NO is rapidly oxidized to nitrite and nitrate, the assumption made for the use of this method is that nitrite concentration is proportional to NO concentration found in a biological sample. Another limitation was towards the nitrate signal. To mimic the wild-type physiological environment of the human skin in our experiments, we decided to avoid the use of bacterial nitrate reductases, which reduce nitrate to nitrite. As such, small proportions of the NO content oxidized to more stable nitrate ions were undetectable using our Griess method. Moreover, Griess reaction assay is a technique relying only on the proportional postulate between nitrite and NO concentrations. Hence, we cannot precisely measure the concentration of nitrite nor NO in a biological sample. We tested this limitation using different concentrations of sodium nitrite (NaNO_2) with our human skin homogenate model. We observed that we could detect and differentiate higher concentrations of nitrite, but we did not obtain the exact concentration of nitrite using the Qunicom NO assay kit (Graph 6). Please note that only one sample was tested for each concentration of NaNO_2 ; thereby, no statistical analysis was computed for this sensitivity test.

Graph 6. NaNO₂ vs Sham



Lastly, since biological samples have a high content of protein and high turbidity, deproteination was imperative to measure the stable azo compound fluorescence with the spectrophotometer. However, the use of the non-acidic precipitation method (i.e. NaOH and ZnSO₄) added to the ultrafiltration, using the Amicon ultra-0.5 centrifugal filter, had trivial effects on our samples. Some proteins that were nitrosated following the photo-release of NO may have been removed during this deproteination step, hence mitigating our results.

However, the Griess reaction assay forms very stable azo compounds that are easier to detect with the spectrophotometer [110] compared to other NO dyes (e.g. DAF-2DA), especially in high turbidity environment, such as a skin homogenate. This stability factor was greatly considered while designing the protocol of these experiments.

The standard curve generated using the included nitrite standards enabled concentrations of NO in the skin homogenate to be estimated for different treatment conditions.

UVA exposure

Unsurprisingly, skin homogenate exposure to UVA released the highest amount of nitrite, corresponding to the fraction of NO liberated from the skin. The highest nitrite concentrations were measured in the first two experiments using light alone or the enzymatic NOS inhibitor L-NMMA.

We anticipated such high values as already reported [12, 15, 16, 64], since the mechanism of action of UVA photons to release NO occurs via a non-enzymatic photolytic process. Therefore, even if the NOSs are blocked by the non-selective NOS inhibitor L-NMMA, NO will be released by the direct effect of light (photodecomposition) on nitrite as well as S-nitrosothiol compounds (RSNO). In the third experiment using the selective NO scavenger C-PTIO, much lower nitrite levels were monitored at 6.99 μM compared to approximately 19 μM in the first two experiments (18.69 μM and 18.45 μM , respectively) post UVA exposure. This clearly demonstrates the power of UVA, capable of releasing skin NO despite the use of a potent NO scavenger.

Red and NIR exposure

Red (660 nm) and near-infrared (850 nm) wavelengths behaved much similarly. Nitrite levels obtained at 660 nm & 850 nm with light alone in the first experiment were much lower than for UVA, revealing approximately half the concentration for both wavelengths. However, 850 nm exhibited slightly higher levels than 660 nm. The possible explanation is the direct thermal effect on NOS triggered by water absorption at 850 nm generating more enzymatic NO release.

In the second and third experiments using an enzymatic NOS inhibitor and a selective NO scavenger, both wavelengths responded much alike. This emphasizes the predominant nature of the enzymatic NO release process (via NOS) when using visible red and near-infrared photons [101]. Even so, we found a statistically significant difference in nitrite levels while blocking NOS by L-NMMA between the sham control and 660 & 850 nm light exposures, supporting the existence of a partial photolytic process. In truth, further studies are needed to prove this hypothesis.

Combined comparison

When comparing experiment 1 (light alone) to experiment 2 (NOS inhibitor L-NMMA), several interesting data arise. First, UVA light (365 nm) reached similar levels of nitrite with or without L-NMMA, asserting that NO release is almost entirely photolytic (non-enzymatic).

Furthermore, the only statistically significant difference in nitrite levels without or with L-NMMA, (experiment #1 vs experiment #2) was at 850 nm, demonstrating that at this wavelength NO release is predominantly enzymatic via NOS activation.

As for the comparison of experiment 1 (light alone) to experiment 3 (selective NO scavenger C-PTIO), the significant fall in nitrite levels when L-NMMA was present following UVA light exposure emphasizes the non-enzymatic (photolytic) importance of this NO release process.

Clinical Aspects

NO derivatives are found in huge amounts in the largest body organ, the skin. This hidden but available cutaneous NO store may reach several hundred folds (250X) the quantity found in blood circulation. What if this vast amount of NO would become available for local or systemic (remote) beneficial effects. Phototherapy using low-intensity light can release NO by non-enzymatic and enzymatic reactions. Ionizing UVA light is known for its strong non-enzymatic (photolytic) capacity to release cutaneous NO. Similarly, blue light can also release NO non-enzymatically. Still, the downsides of UVA and blue light are photoaging and persistent hyperpigmentation. On the other hand, safer non-ionizing wavelengths in the red and NIR spectra (as part of photobiomodulation) have not yet been described as NO release promoters. Our Griess assay data suggest that the primary NO release mechanism for these safer wavelengths is enzymatic via NOS activation. The clinical implications of this discovery are considerable, especially in wound healing processes and remote body organ beneficial effects (i.e. reduction blood pressure) without

cutaneous side effects. Further clinical studies are needed to assess local and systemic effects consecutive to NO release coming from the skin, such as *in vivo* quantification of nitric oxide (NO) release from intact human skin following exposure to photobiomodulation wavelengths in the visible and near-infrared spectrum measured by chemiluminescence detection. The same measurement method could also be used after large surface exposure followed by serum nitric oxide (NO) analysis while monitoring cardiovascular parameters / endothelial function systemic effects.

Next steps

I intend to pursue further work on the mechanisms inducing a favourable cellular response in humans and bi-lamellar reconstructed skin (BRS) through NO release. It represents an incredible opportunity for the well-being of victims with severe burns who currently suffer from long waiting periods before obtaining their BRS transplant and perhaps even improving their healing process light treatments following BRP-transplantation.

Conclusion

PBM is an emerging branch of phototherapy using visible light and near IR wavelengths. Among several known effector molecules regulated by PBM, NO seems to have a pivotal role. The two-sided nature of NO effect in the skin likely provides fascinating protective effects. Systemic effects impacting distant organs are also possible.

We demonstrated that NIR and red wavelengths are capable of releasing NO in the skin using a colorimetric Griess assay enzymatically, presumably via NOSs after measuring NO levels from ex-vivo human skin. We also showed that UVA effectively releases NO essentially by a photolytic (non-enzymatic) reaction by the use of non-selective and selective molecular NOS inhibitors, such

as L-NMMA and the NO scavenger C-PTIO, respectively. Finally, we report the superior enzymatic effect (likely temperature-dependent) of NIR at 850nm, releasing statistically less NO than red light in the presence of L-NMMA. This is consistent with the fact that red photons (660nm) are slightly more energetic than NIR photons (850nm), providing more photolytic capabilities bearing in mind that the effect is mainly enzymatic at 660nm.

This is another piece of the puzzle to better understand basic NO-related mechanisms following the use of low intensity light exposure in skin applications. Researchers' curiosity, serendipity, passion, and hard work will continue to answer unanswered questions, and thereby fundamentally expand our knowledge in PBM.

References

- [1] S. Moncada, and A. Higgs, "The L-arginine-nitric oxide pathway," *N Engl J Med*, 329(27), 2002-12 (1993).
- [2] J. E. Baudouin, and P. Tachon, "Constitutive nitric oxide synthase is present in normal human keratinocytes," *J Invest Dermatol*, 106(3), 428-31 (1996).
- [3] C. Oplander, and C. V. Suschek, "New aspects of nitrite homeostasis in human skin," *J Invest Dermatol*, 129(4), 820-2 (2009).
- [4] J. D. Luo, and A. F. Chen, "Nitric oxide: a newly discovered function on wound healing," *Acta Pharmacol Sin*, 26(3), 259-64 (2005).
- [5] Y. Shimizu, M. Sakai, Y. Umemura *et al.*, "Immunohistochemical localization of nitric oxide synthase in normal human skin: expression of endothelial-type and inducible-type nitric oxide synthase in keratinocytes," *J Dermatol*, 24(2), 80-7 (1997).
- [6] S. Frank, H. Kampfer, C. Wetzler *et al.*, "Nitric oxide drives skin repair: novel functions of an established mediator," *Kidney Int*, 61(3), 882-8 (2002).
- [7] J. W. Coleman, "Nitric oxide: a regulator of mast cell activation and mast cell-mediated inflammation," *Clin Exp Immunol*, 129(1), 4-10 (2002).
- [8] F. Violi, R. Marino, M. T. Milite *et al.*, "Nitric oxide and its role in lipid peroxidation," *Diabetes Metab Res Rev*, 15(4), 283-8 (1999).
- [9] A. Ayala, M. F. Muñoz, and S. Argüelles, "Lipid peroxidation: production, metabolism, and signaling mechanisms of malondialdehyde and 4-hydroxy-2-nonenal," *Oxid Med Cell Longev*, 2014, 360438 (2014).
- [10] M. Mowbray, S. McLintock, R. Weerakoon *et al.*, "Enzyme-independent NO stores in human skin: quantification and influence of UV radiation," *J Invest Dermatol*, 129(4), 834-42 (2009).
- [11] C. V. Suschek, [Nitric Oxide Derivatives and Skin Environmental Exposure to Light: From Molecular Pathways to Therapeutic Opportunities] Springer International Publishing, Cham(2016).
- [12] C. Oplander, and C. V. Suschek, "The Role of Photolabile Dermal Nitric Oxide Derivates in Ultraviolet Radiation (UVR)-Induced Cell Death," *Int J Mol Sci*, 14(1), 191-204 (2012).
- [13] A. N. Paunel, A. Dejam, S. Thelen *et al.*, "Enzyme-independent nitric oxide formation during UVA challenge of human skin: characterization, molecular sources, and mechanisms," *Free Radic Biol Med*, 38(5), 606-15 (2005).
- [14] D. Liu, B. O. Fernandez, A. Hamilton *et al.*, "UVA irradiation of human skin vasodilates arterial vasculature and lowers blood pressure independently of nitric oxide synthase," *J Invest Dermatol*, 134(7), 1839-46 (2014).
- [15] C. V. Suschek, C. Oplander, and E. E. van Faassen, "Non-enzymatic NO production in human skin: effect of UVA on cutaneous NO stores," *Nitric Oxide*, 22(2), 120-35 (2010).
- [16] C. Oplander, M. Baschin, E. E. van Faassen *et al.*, "A new method for sustained generation of ultrapure nitric oxide-containing gas mixtures via controlled UVA-photolysis of nitrite solutions," *Nitric Oxide*, 23(4), 275-83 (2010).
- [17] J. Rodriguez, R. E. Maloney, T. Rassaf *et al.*, "Chemical nature of nitric oxide storage forms in rat vascular tissue," *Proc Natl Acad Sci U S A*, 100(1), 336-41 (2003).
- [18] C. Oplander, A. Deck, C. M. Volkmar *et al.*, "Mechanism and biological relevance of blue-light (420-453 nm)-induced nonenzymatic nitric oxide generation from photolabile nitric oxide derivates in human skin in vitro and in vivo," *Free Radic Biol Med*, 65, 1363-77 (2013).
- [19] Z. C. F. Garza, M. Born, P. A. J. Hilbers *et al.*, "Visible Blue Light Therapy: Molecular Mechanisms and Therapeutic Opportunities," *Current Medicinal Chemistry*, 25(40), 5564-5577 (2018).
- [20] M. Stern, M. Broja, R. Sansone *et al.*, "Blue light exposure decreases systolic blood pressure, arterial stiffness, and improves endothelial function in humans," *Eur J Prev Cardiol*, 25(17), 1875-1883 (2018).

- [21] D. Barolet, and G. Cormack, "Photobiomodulation of NO bioactivity and release in the skin," *Lasers Surg Med*, 49(S28), 54 (2017).
- [22] A. Barolet, G. Cormack, and D. Barolet, "Measurement of Light-Induced Nitric Oxide Release from Ex Vivo Skin Homogenate Using a Colorimetric Nitrite Assay (Griess Assay)," *Skin Research Group of Canada Annual Conference*, (2018).
- [23] S. Moskvina, E. Askhadulin, and A. Kochetkov, "Low-Level Laser Therapy in Prevention of the Development of Endothelial Dysfunction and Clinical Experience of Treatment and Rehabilitation of COVID-19 Patients," *Rehabilitation Research and Practice*, 2021, 6626932 (2021).
- [24] C. Opländer, A. Deck, C. M. Volkmar *et al.*, "Mechanism and biological relevance of blue-light (420-453 nm)-induced nonenzymatic nitric oxide generation from photolabile nitric oxide derivatives in human skin in vitro and in vivo," *Free radical biology & medicine*, 65, 1363-1377 (2013).
- [25] A. C. Barolet, G. Cormack, G. Lachance *et al.*, "In vivo quantification of nitric oxide (NO) release from intact human skin following exposure to photobiomodulation wavelengths in the visible and near infrared spectrum," *SPIE BiOS*, 10861, (2019).
- [26] M. Feelisch, V. Kolb-Bachofen, D. Liu *et al.*, "Is sunlight good for our heart?," *Eur Heart J*, 31(9), 1041-5 (2010).
- [27] C. Monaghan, L. C. McIlvenna, L. Liddle *et al.*, "The effects of two different doses of ultraviolet-A light exposure on nitric oxide metabolites and cardiorespiratory outcomes," *Eur J Appl Physiol*, 118(5), 1043-1052 (2018).
- [28] D. J. Muggeridge, N. Sculthorpe, F. M. Grace *et al.*, "Acute whole body UVA irradiation combined with nitrate ingestion enhances time trial performance in trained cyclists," *Nitric Oxide*, 48, 3-9 (2015).
- [29] R. Weller, "Nitric oxide: a key mediator in cutaneous physiology," *Clin Exp Dermatol*, 28(5), 511-4 (2003).
- [30] R. Weller, "Nitric oxide--a newly discovered chemical transmitter in human skin," *Br J Dermatol*, 137(5), 665-72 (1997).
- [31] R. Weller, and A. Ormerod, "Increased expression of inducible nitric oxide (NO) synthase," *Br J Dermatol*, 136(1), 136-7 (1997).
- [32] R. Weller, T. Billiar, and Y. Vodovotz, "Pro- and anti-apoptotic effects of nitric oxide in irradiated keratinocytes: the role of superoxide," *Skin Pharmacol Appl Skin Physiol*, 15(5), 348-52 (2002).
- [33] C. V. Suschek, O. Schnorr, and V. Kolb-Bachofen, "The role of iNOS in chronic inflammatory processes in vivo: is it damage-promoting, protective, or active at all?," *Curr Mol Med*, 4(7), 763-75 (2004).
- [34] Y. Xu, Y. Shao, J. Zhou *et al.*, "Ultraviolet irradiation-induces epidermal growth factor receptor (EGFR) nuclear translocation in human keratinocytes," *J Cell Biochem*, 107(5), 873-80 (2009).
- [35] Q.-M. Hu, W.-J. Yi, M.-Y. Su *et al.*, "Induction of retinal-dependent calcium influx in human melanocytes by UVA or UVB radiation contributes to the stimulation of melanosome transfer," *Cell Proliferation*, 50(6), e12372 (2017).
- [36] M. M. Cals-Grierson, and A. D. Ormerod, "Nitric oxide function in the skin," *Nitric Oxide*, 10(4), 179-93 (2004).
- [37] J. M. Powers, and J. E. J. Murphy, "Sunlight radiation as a villain and hero: 60 years of illuminating research," *Int J Radiat Biol*, 95(7), 1043-1049 (2019).
- [38] C. V. Suschek, K. Briviba, D. Bruch-Gerharz *et al.*, "Even after UVA-exposure will nitric oxide protect cells from reactive oxygen intermediate-mediated apoptosis and necrosis," *Cell Death Differ*, 8(5), 515-27 (2001).
- [39] K. M. Miranda, M. G. Espey, D. Jourdain *et al.*, [Chapter 3 - The Chemical Biology of Nitric Oxide] *Academic Press*, San Diego(2000).
- [40] C. V. Suschek, A. Paunel, and V. Kolb-Bachofen, "Nonenzymatic nitric oxide formation during UVA irradiation of human skin: experimental setups and ways to measure," *Methods Enzymol*, 396, 568-78 (2005).

- [41] M. Kirsch, and H. de Groot, "Formation of Peroxynitrite from Reaction of Nitroxyl Anion with Molecular Oxygen *," *Journal of Biological Chemistry*, 277(16), 13379-13388 (2002).
- [42] A. Treinin, and E. Hayon, "Absorption spectra and reaction kinetics of NO₂, N₂O₃, and N₂O₄ in aqueous solution," *Journal of the American Chemical Society*, 92(20), 5821-5828 (1970).
- [43] M. M. Veleparampil, U. K. Aravind, and C. T. Aravindakumar, "Decomposition of S-Nitrosothiols Induced by UV and Sunlight," *Advances in Physical Chemistry*, 2009, 5 (2009).
- [44] S. M. Shishido, and M. G. de Oliveira, "Polyethylene glycol matrix reduces the rates of photochemical and thermal release of nitric oxide from S-nitroso-N-acetylcysteine," *Photochem Photobiol*, 71(3), 273-80 (2000).
- [45] G. Holliman, D. Lowe, H. Cohen *et al.*, "Ultraviolet Radiation-Induced Production of Nitric Oxide: A multi-cell and multi-donor analysis," *Sci Rep*, 7(1), 11105 (2017).
- [46] A. Dejam, P. Kleinbongard, T. Rassaf *et al.*, "Thiols enhance NO formation from nitrate photolysis," *Free Radic Biol Med*, 35(12), 1551-9 (2003).
- [47] B. Sander, P. Rasmussen, and A. Fredenslund, "Calculation of solid-liquid equilibria in aqueous solutions of nitrate salts using an extended UNIQUAC equation," *Chemical Engineering Science*, 41(5), 1197-1202 (1986).
- [48] S. Pfaff, J. Liebmann, M. Born *et al.*, "Prospective Randomized Long-Term Study on the Efficacy and Safety of UV-Free Blue Light for Treating Mild Psoriasis Vulgaris," *Dermatology*, 231(1), 24-34 (2015).
- [49] K. Keemss, S. C. Pfaff, M. Born *et al.*, "Prospective, Randomized Study on the Efficacy and Safety of Local UV-Free Blue Light Treatment of Eczema," *Dermatology*, 232(4), 496-502 (2016).
- [50] Y. Nakashima, S. Ohta, and A. M. Wolf, "Blue light-induced oxidative stress in live skin," *Free Radic Biol Med*, 108, 300-310 (2017).
- [51] B. F. Godley, F. A. Shamsi, F. Q. Liang *et al.*, "Blue light induces mitochondrial DNA damage and free radical production in epithelial cells," *J Biol Chem*, 280(22), 21061-6 (2005).
- [52] S. Vandersee, M. Beyer, J. Lademann *et al.*, "Blue-Violet Light Irradiation Dose Dependently Decreases Carotenoids in Human Skin, Which Indicates the Generation of Free Radicals," *Oxidative Medicine and Cellular Longevity*, 2015, 579675 (2015).
- [53] T. Passeron, "Melasma pathogenesis and influencing factors - an overview of the latest research," *J Eur Acad Dermatol Venereol*, 27 Suppl 1, 5-6 (2013).
- [54] E. Dupont, J. Gomez, and D. Bilodeau, "Beyond UV radiation: a skin under challenge," *Int J Cosmet Sci*, 35(3), 224-32 (2013).
- [55] B. H. Mahmoud, E. Ruvoilo, C. L. Hexsel *et al.*, "Impact of long-wavelength UVA and visible light on melanocompetent skin," *J Invest Dermatol*, 130(8), 2092-7 (2010).
- [56] A. H. Huang, and A. L. Chien, "Photoaging: a Review of Current Literature," *Current Dermatology Reports*, 9(1), 22-29 (2020).
- [57] J. Liebmann, M. Born, and V. Kolb-Bachofen, "Blue-light irradiation regulates proliferation and differentiation in human skin cells," *J Invest Dermatol*, 130(1), 259-69 (2010).
- [58] L. Taflinski, E. Demir, J. Kauczok *et al.*, "Blue light inhibits transforming growth factor- β 1-induced myofibroblast differentiation of human dermal fibroblasts," *Exp Dermatol*, 23(4), 240-6 (2014).
- [59] A. Becker, C. Sticht, H. Dweep *et al.*, [Impact of blue LED irradiation on proliferation and gene expression of cultured human keratinocytes] *SPIE, PWB* (2015).
- [60] K. Taoufik, E. Mavrogonatou, T. Eliades *et al.*, "Effect of blue light on the proliferation of human gingival fibroblasts," *Dental materials : official publication of the Academy of Dental Materials*, 24(7), 895-900 (2008).
- [61] C. Oplander, S. Hidding, F. B. Werners *et al.*, "Effects of blue light irradiation on human dermal fibroblasts," *J Photochem Photobiol B*, 103(2), 118-25 (2011).
- [62] R. Ankri, H. Friedman, N. Savion *et al.*, "Visible light induces nitric oxide (NO) formation in sperm and endothelial cells," *Lasers Surg Med*, 42(4), 348-52 (2010).
- [63] P. Caraceni, M. Tufoni, and M. E. Bonavita, "Clinical use of albumin," *Blood Transfus*, 11 Suppl 4(Suppl 4), s18-25 (2013).

- [64] C. Oplander, C. M. Volkmar, A. Paunel-Gorgulu *et al.*, “Whole body UVA irradiation lowers systemic blood pressure by release of nitric oxide from intracutaneous photolabile nitric oxide derivatives,” *Circ Res*, 105(10), 1031-40 (2009).
- [65] C. Regazzetti, L. Sormani, D. Debayle *et al.*, “Melanocytes Sense Blue Light and Regulate Pigmentation through Opsin-3,” *Journal of Investigative Dermatology*, 138(1), 171-178 (2018).
- [66] J. G. Coats, B. Maktabi, M. S. Abou-Dahech *et al.*, “Blue Light Protection, Part I—Effects of blue light on the skin,” *Journal of Cosmetic Dermatology*, n/a(n/a).
- [67] J. M. Krassovka, C. V. Suschek, M. Prost *et al.*, “The impact of non-toxic blue light (453 nm) on cellular antioxidative capacity, TGF- β 1 signaling, and myofibrogenesis of human skin fibroblasts,” *Journal of Photochemistry and Photobiology B: Biology*, 209, 111952 (2020).
- [68] I. Albers, E. Zernickel, M. Stern *et al.*, “Blue light (λ =453nm) nitric oxide dependently induces beta-endorphin production of human skin keratinocytes in-vitro and increases systemic beta-endorphin levels in humans in-vivo,” *Free Radic Biol Med*, 145, 78-86 (2019).
- [69] E. Austin, A. N. Geisler, J. Nguyen *et al.*, “Visible light. Part I: Properties and cutaneous effects of visible light,” *J Am Acad Dermatol*, 84(5), 1219-1231 (2021).
- [70] D. Barolet, “Photobiomodulation in Dermatology: Harnessing Light from Visible to Near Infrared,” *Medical Research Archives*, 6(1), 30 (2018).
- [71] A. N. Geisler, E. Austin, J. Nguyen *et al.*, “Visible light. Part II: Photoprotection against visible and ultraviolet light,” *J Am Acad Dermatol*, 84(5), 1233-1244 (2021).
- [72] A. Mamalis, E. Koo, M. Garcha *et al.*, “High fluence light emitting diode-generated red light modulates characteristics associated with skin fibrosis,” *J Biophotonics*, 9(11-12), 1167-1179 (2016).
- [73] A. Mamalis, and J. Jagdeo, “High-Fluence Light-Emitting Diode-Generated Red Light Modulates the Transforming Growth Factor-Beta Pathway in Human Skin Fibroblasts,” *Dermatol Surg*, 44(10), 1317-1322 (2018).
- [74] L. F. de Freitas, and M. R. Hamblin, “Proposed Mechanisms of Photobiomodulation or Low-Level Light Therapy,” *IEEE J Sel Top Quantum Electron*, 22(3), (2016).
- [75] D. Barolet, F. Christiaens, and M. R. Hamblin, “Infrared and skin: Friend or foe,” *J Photochem Photobiol B*, 155, 78-85 (2016).
- [76] P. Schroeder, J. Lademann, M. E. Darvin *et al.*, “Infrared radiation-induced matrix metalloproteinase in human skin: implications for protection,” *J Invest Dermatol*, 128(10), 2491-7 (2008).
- [77] P. Schroeder, C. Calles, and J. Krutmann, “Prevention of infrared-A radiation mediated detrimental effects in human skin,” *Skin Therapy Lett*, 14(5), 4-5 (2009).
- [78] S. M. Schieke, P. Schroeder, and J. Krutmann, “Cutaneous effects of infrared radiation: from clinical observations to molecular response mechanisms,” *Photodermatol Photoimmunol Photomed*, 19(5), 228-34 (2003).
- [79] J. Halper, A. Griffin, W. Hu *et al.*, “In vitro culture decreases the expression of TGF(β), Hsp47 and type I procollagen and increases the expression of CTGF in avian tendon explants,” *J Musculoskelet Neuronal Interact*, 5(1), 53-63 (2005).
- [80] S. Schieke, H. Stege, V. Kurten *et al.*, “Infrared-A radiation-induced matrix metalloproteinase 1 expression is mediated through extracellular signal-regulated kinase 1/2 activation in human dermal fibroblasts,” *J Invest Dermatol*, 119(6), 1323-9 (2002).
- [81] G. M. Halliday, “Activation of molecular adaptation to sunlight--a new approach to photoprotection,” *J Invest Dermatol*, 125(5), xviii-xix (2005).
- [82] G. Schauburger, H. Maier, A. Cabaj *et al.*, “Evaluation of the goodness of fit of solar simulated radiation to a reference solar spectrum for photobiological experiments,” *Med Phys*, 31(9), 2509-19 (2004).
- [83] H. Piazena, and D. Kelleher, “Comments on "Cellular response to infrared radiation involves retrograde mitochondrial signaling",” *Free Radic Biol Med*, 44(10), 1869; author reply 1870-1 (2008).

- [84] C. Marionnet, C. Pierrard, F. Lejeune *et al.*, "Different Oxidative Stress Response in Keratinocytes and Fibroblasts of Reconstructed Skin Exposed to Non Extreme Daily-Ultraviolet Radiation," PLoS ONE, 5(8), e12059 (2010).
- [85] C. Marionnet, C. Tricaud, and F. Bernerd, "Exposure to Non-Extreme Solar UV Daylight: Spectral Characterization, Effects on Skin and Photoprotection," International Journal of Molecular Sciences, 16(1), 68-90 (2014).
- [86] P. Avci, A. Gupta, M. Sadasivam *et al.*, "Low-level laser (light) therapy (LLLT) in skin: stimulating, healing, restoring," Semin Cutan Med Surg, 32(1), 41-52 (2013).
- [87] M. R. Hamblin, "Mechanisms and applications of the anti-inflammatory effects of photobiomodulation," AIMS Biophys, 4(3), 337-361 (2017).
- [88] A. Gupta, T. Dai, and M. R. Hamblin, "Effect of red and near-infrared wavelengths on low-level laser (light) therapy-induced healing of partial-thickness dermal abrasion in mice," Lasers Med Sci, 29(1), 257-65 (2014).
- [89] F. Vatansever, and M. R. Hamblin, "Far infrared radiation (FIR): its biological effects and medical applications," Photonics Lasers Med, 4, 255-266 (2012).
- [90] H. Chung, T. Dai, S. K. Sharma *et al.*, "The nuts and bolts of low-level laser (light) therapy," Ann Biomed Eng, 40(2), 516-33 (2012).
- [91] M. R. Hamblin, M. V. Pires de Sousa, P. R. Arany *et al.*, "Low level laser (light) therapy and photobiomodulation: the path forward." 9309, 930902-930902-11.
- [92] M. Hamblin, [The role of nitric oxide in low level light therapy] SPIE, PWB (2008).
- [93] M. R. Hamblin, "Introduction to experimental and clinical studies using low-level laser (light) therapy (LLLT)," Lasers Surg Med, 42(6), 447-9 (2010).
- [94] N. L. Lohr, A. Keszler, P. Pratt *et al.*, "Enhancement of nitric oxide release from nitrosyl hemoglobin and nitrosyl myoglobin by red/near infrared radiation: potential role in cardioprotection," J Mol Cell Cardiol, 47(2), 256-63 (2009).
- [95] A. Zielke, [Photo-excitation of electrons in cytochrome c oxidase as a theory of the mechanism of the increase of ATP production in mitochondria by laser therapy] SPIE, PWB (2014).
- [96] M. R. Blomberg, "Mechanism of Oxygen Reduction in Cytochrome c Oxidase and the Role of the Active Site Tyrosine," Biochemistry, 55(3), 489-500 (2016).
- [97] A. Amaroli, S. Ferrando, and S. Benedicenti, "Photobiomodulation Affects Key Cellular Pathways of all Life-Forms: Considerations on Old and New Laser Light Targets and the Calcium Issue," Photochemistry and Photobiology, 95(1), 455-459 (2019).
- [98] E. Alexandratou, D. Yova, P. Handris *et al.*, "Human fibroblast alterations induced by low power laser irradiation at the single cell level using confocal microscopy," Photochem Photobiol Sci, 1(8), 547-52 (2002).
- [99] I. N. Mungrue, and D. S. Bredt, "nNOS at a glance: implications for brain and brawn," Journal of Cell Science, 117(13), 2627-2629 (2004).
- [100] J. Qian, and D. Fulton, "Post-translational regulation of endothelial nitric oxide synthase in vascular endothelium," Frontiers in Physiology, 4(347), (2013).
- [101] M. Rizzi, M. Migliario, S. Tonello *et al.*, "Photobiomodulation induces in vitro re-epithelialization via nitric oxide production," Lasers Med Sci, 33(5), 1003-1008 (2018).
- [102] M. G. Mason, P. Nicholls, and C. E. Cooper, "Re-evaluation of the near infrared spectra of mitochondrial cytochrome c oxidase: Implications for non invasive in vivo monitoring of tissues," Biochim Biophys Acta, 1837(11), 1882-1891 (2014).
- [103] M. Averna, R. Stifanese, R. De Tullio *et al.*, "In vivo degradation of nitric oxide synthase (NOS) and heat shock protein 90 (HSP90) by calpain is modulated by the formation of a NOS-HSP90 heterocomplex," The FEBS Journal, 275(10), 2501-2511 (2008).
- [104] Y. Osawa, E. R. Lowe, A. C. Everett *et al.*, "Proteolytic degradation of nitric oxide synthase: effect of inhibitors and role of hsp90-based chaperones," J Pharmacol Exp Ther, 304(2), 493-7 (2003).
- [105] H. Kojima, K. Sakurai, K. Kikuchi *et al.*, "Development of a fluorescent indicator for nitric oxide based on the fluorescein chromophore," Chem Pharm Bull (Tokyo), 46(2), 373-5 (1998).

- [106] Y. Gabe, Y. Urano, K. Kikuchi *et al.*, “Highly sensitive fluorescence probes for nitric oxide based on boron dipyrromethene chromophore-rational design of potentially useful bioimaging fluorescence probe,” *J Am Chem Soc*, 126(10), 3357-67 (2004).
- [107] A. Diaspro, P. Bianchini, F. Cella Zanacchi *et al.*, [Confocal Laser Scanning Fluorescence Microscopy] Springer Berlin Heidelberg, Berlin, Heidelberg(2013).
- [108] M. Gerboles, F. Lagler, D. Rembges *et al.*, “Assessment of uncertainty of NO₂ measurements by the chemiluminescence method and discussion of the quality objective of the NO₂ European Directive,” *J Environ Monit*, 5(4), 529-40 (2003).
- [109] A. Wany, A. K. Gupta, A. Kumari *et al.*, [Chemiluminescence Detection of Nitric Oxide from Roots, Leaves, and Root Mitochondria] Springer New York, New York, NY(2016).
- [110] J. Sun, X. Zhang, M. Broderick *et al.*, “Measurement of Nitric Oxide Production in Biological Systems by Using Griess Reaction Assay,” *Sensors*, 3(8), 276-284 (2003).
- [111] P. Griess, “Bemerkungen zu der Abhandlung der HH. Weselsky und Benedikt „Ueber einige Azoverbindungen”,” *Berichte der deutschen chemischen Gesellschaft*, 12(1), 426-428 (1879).
- [112] C. P. Verdon, B. A. Burton, and R. L. Prior, “Sample pretreatment with nitrate reductase and glucose-6-phosphate dehydrogenase quantitatively reduces nitrate while avoiding interference by NADP⁺ when the Griess reaction is used to assay for nitrite,” *Anal Biochem*, 224(2), 502-8 (1995).
- [113] I. Guevara, J. Iwanejko, A. Dembińska-Kieć *et al.*, “Determination of nitrite/nitrate in human biological material by the simple Griess reaction,” *Clin Chim Acta*, 274(2), 177-88 (1998).
- [114] T. Rassaf, U. Flogel, C. Drexhage *et al.*, “Nitrite reductase function of deoxymyoglobin: oxygen sensor and regulator of cardiac energetics and function,” *Circ Res*, 100(12), 1749-54 (2007).
- [115] C. Opländer, M. M. Cortese, H. G. Korth *et al.*, “The impact of nitrite and antioxidants on ultraviolet-A-induced cell death of human skin fibroblasts,” *Free Radic Biol Med*, 43(5), 818-29 (2007).
- [116] K. D. Kroncke, K. Fehsel, and V. Kolb-Bachofen, “Nitric oxide: cytotoxicity versus cytoprotection-how, why, when, and where?,” *Nitric Oxide*, 1(2), 107-20 (1997).
- [117] C. V. Suschek, P. Schroeder, O. Aust *et al.*, “The presence of nitrite during UVA irradiation protects from apoptosis,” *FASEB J*, 17(15), 2342-4 (2003).
- [118] C. Oplander, M. M. Cortese, H. G. Korth *et al.*, “The impact of nitrite and antioxidants on ultraviolet-A-induced cell death of human skin fibroblasts,” *Free Radic Biol Med*, 43(5), 818-29 (2007).
- [119] R. C. Mosca, A. A. Ong, O. Albasha *et al.*, “Photobiomodulation Therapy for Wound Care: A Potent, Noninvasive, Photocutaneous Approach,” *Adv Skin Wound Care*, 32(4), 157-167 (2019).
- [120] Y. Moriyama, J. Nguyen, M. Akens *et al.*, “In vivo effects of low level laser therapy on inducible nitric oxide synthase,” *Lasers Surg Med*, 41(3), 227-31 (2009).
- [121] B. Meloun, L. Morávek, and V. Kostka, “Complete amino acid sequence of human serum albumin,” *FEBS Letters*, 58(1), 134-137 (1975).
- [122] T. Münzel, M. Sørensen, T. Gori *et al.*, “Environmental stressors and cardio-metabolic disease: part I-epidemiologic evidence supporting a role for noise and air pollution and effects of mitigation strategies,” *Eur Heart J*, 38(8), 550-556 (2017).
- [123] D. Luo, Y. Cheng, H. Zhang *et al.*, “Association between high blood pressure and long term cardiovascular events in young adults: systematic review and meta-analysis,” *BMJ*, 370, m3222 (2020).
- [124] R. B. Weller, Y. Wang, J. He *et al.*, “Does Incident Solar Ultraviolet Radiation Lower Blood Pressure?,” *Journal of the American Heart Association*, 9(5), e013837 (2020).
- [125] R. B. Weller, “Sunlight Has Cardiovascular Benefits Independently of Vitamin D,” *Blood Purif*, 41(1-3), 130-4 (2016).
- [126] G. Rose, “Seasonal Variation in Blood Pressure in Man,” *Nature*, 189(4760), 235-235 (1961).
- [127] P. J. Brennan, G. Greenberg, W. E. Miall *et al.*, “Seasonal variation in arterial blood pressure,” *Br Med J (Clin Res Ed)*, 285(6346), 919-23 (1982).

- [128] Y. Imai, M. Munakata, I. Tsuji *et al.*, “Seasonal variation in blood pressure in normotensive women studied by home measurements,” *Clin Sci (Lond)*, 90(1), 55-60 (1996).
- [129] T. Iwahori, K. Miura, K. Obayashi *et al.*, “Seasonal variation in home blood pressure: findings from nationwide web-based monitoring in Japan,” *BMJ Open*, 8(1), e017351 (2018).
- [130] S. G. Rostand, “Ultraviolet light may contribute to geographic and racial blood pressure differences,” *Hypertension*, 30(2 Pt 1), 150-6 (1997).
- [131] R. F. Furchgott, S. J. Ehrreich, and E. Greenblatt, “The photoactivated relaxation of smooth muscle of rabbit aorta,” *J Gen Physiol*, 44, 499-519 (1961).
- [132] J. O. Lundberg, E. Weitzberg, and M. T. Gladwin, “The nitrate-nitrite-nitric oxide pathway in physiology and therapeutics,” *Nat Rev Drug Discov*, 7(2), 156-67 (2008).
- [133] R. L. Toma, M. X. Oliveira, A. C. M. Renno *et al.*, “Photobiomodulation (PBM) therapy at 904 nm mitigates effects of exercise-induced skeletal muscle fatigue in young women,” *Lasers in Medical Science*, 33(6), 1197-1205 (2018).
- [134] J. T. Hashmi, Y.-Y. Huang, B. Z. Osmani *et al.*, “Role of Low-Level Laser Therapy in Neurorehabilitation,” *PM & R : the journal of injury, function, and rehabilitation*, 2(12 Suppl 2), S292-S305 (2010).
- [135] F. Michel, and D. Barolet, “A new visual analog scale to measure distinctive well-being effects of LED Photobiomodulation,” *SPIE Proceedings*, 9695(96950N-96950N-11), (2016).
- [136] G. Lorzynski, C. V. Suschek, and V. Kolb-Bachofen, “In hepatocytes the regulation of NOS-2 activity at physiological L-arginine levels suggests a close link to the urea cycle,” *Nitric Oxide*, 14(4), 300-8 (2006).